Research Article

Early Pleistocene upper bathyal communities in fault-bounded paleovalleys of the island of Rhodes (Greece)

Pierre Moissette[a] [iD], Frédéric Quillévéré[b] [iD], George Kontakiotis[a], Danae Thivaiou[a,c,d] [iD], Efterpi Koskeridou[a] [iD], Assimina Antonarakou[a] [iD], Hara Drinia[a] [iD], Mihaela Melinte-Dobrinescu[e] and Jean-Jacques Cornée[f] [iD]

[a]Faculty of Geology and Geoenvironment, School of Earth Sciences, Department of Historical Geology-Paleontology, National and Kapodistrian University of Athens, Panepistimiopolis, Zografou, 15784, Athens, Greece; [b]Univ. Lyon, Université Claude Bernard Lyon 1, ENS de Lyon, CNRS, UMR 5276 LGL-TPE, F-69622, Villeurbanne, France; [c]Géosciences Montpellier, UMR 5243, Department of Geology, Université des Antilles, Campus de Fouillole, 97159 Pointe à Pitre, Guadeloupe; [d]Naturhistorisches Museum Basel, Augustinergasse 2, 4051, Basel, Switzerland; [e]National Institute of Marine Geology and Geoecology, 23–25 Dimitrie Onciul Street, PO Box 34–51, 70318 Bucharest, Romania and [f]Géosciences Montpellier, UMR CNRS 5243, Université des Antilles-Université Montpellier 2, place Eugène-Bataillon, CC 060, 34095 Montpellier Cedex 05, France

Abstract

Two sediment sections are investigated at Cape Arkhangelos, island of Rhodes, where Pleistocene marine sediments crop out in horsts and grabens of a Mesozoic basement. There, hemipelagic sediments characterized by upper bathyal communities are atypically mixed with much shallower faunal components because they were deposited close to rugged coastal landforms. Biostratigraphic analyses show that the sections were deposited between 1.8 and 0.9 Ma, and between 1.8 and 1.6 Ma, respectively. By combining the planktonic/benthic foraminiferal ratio with 31 bathymetric indicators chosen among extant species of benthic foraminifera, mollusks, and bryozoans, we show that relative sea-level fluctuations can be reconstructed in these atypical settings despite the proximity of steep slopes that favored transportation of allochthonous fauna. The shallow-water components (including gravels and calcareous algae) were transported downslope by the combined action of gravity, currents, and tectonic disturbance that promoted drowning (with a maximum flooding recorded at ca. 1.7 Ma) and then uplift of fault-bounded paleovalleys that formed during the Early Pleistocene. Abrupt facies changes and age differences between sections have been triggered by the irregular paleotopography of the Mesozoic basement, which fostered differential depositional settings, with outer to middle neritic deposits above the horsts and upper bathyal deposits in paleovalleys.

Keywords: Foraminifera, Mollusks, Bryozoans, Calcareous nannofossils, Tectonics, Pleistocene, Rhodes, Aegean

Introduction

The Greek island of Rhodes is situated in the southeastern part of the Aegean Sea, an embayment of the Mediterranean Sea (Fig. 1A). Because of substantial Late Pleistocene and Holocene vertical tectonic movements, the Pleistocene, mostly characterized by marine deposits, largely crop out (Fig. 1B) along its eastern coast (e.g., Mutti et al., 1970; Hanken et al., 1996; van Hinsbergen et al., 2007; Cornée et al., 2019). Especially during the last two decades, intensive research has provided a great amount of information about the sedimentology, stratigraphy, and paleontology of these richly fossiliferous strata.

The Pleistocene sediments of Rhodes were emplaced in steep-flanked paleovalleys of the deformed Mesozoic basement of the Aegean forearc and consequently comprise a variety of facies (e.g., Meulenkamp et al., 1972; Hanken et al., 1996; Titschack et al., 2013). They were deposited at water depths between the sea surface (and even in rivers and lagoons) and the upper bathyal. A revised stratigraphic subdivision of the Pleistocene has been proposed by Titschack et al. (2013), Quillévéré et al. (2016), and Cornée et al. (2019). Ten sedimentary formations (included in five synthems) have thus been defined. Among these formations, the deep-water Lindos Bay Formation, within the Rhodes Synthem, offers a unique sedimentary archive available inland to study the rich upper bathyal foraminiferal and invertebrate communities and to reconstruct the faunal and paleoenvironmental changes that occurred in the eastern Mediterranean during the Early Pleistocene.

Cape Arkhangelos is located in the central-eastern region of the island, about 30 km south of the capital city (Fig. 1B). Two new sections situated very near the seashore have been found and studied in this region (Fig. 1C), because they exhibit facies and fossil contents that appear atypical at Rhodes. The hemipelagic sedimentary deposits of the Lindos Bay Formation usually exhibit predominant but rare upper bathyal organisms, deposited in mostly calm conditions at as much as several hundred meters water depths within homogenous clays (Moissette and Spjeldnaes, 1995; Hanken et al., 1996; Thomsen et al., 2001; Milker et al., 2017; Quillévéré et al., 2019). In the Cape Arkhangelos area, however, deposits of the Lindos Bay Formation are characterized by rich invertebrate faunas often associated with coralline algae and gravels (even pebbles) that are always encrusted by calcareous epibionts and bioeroded.
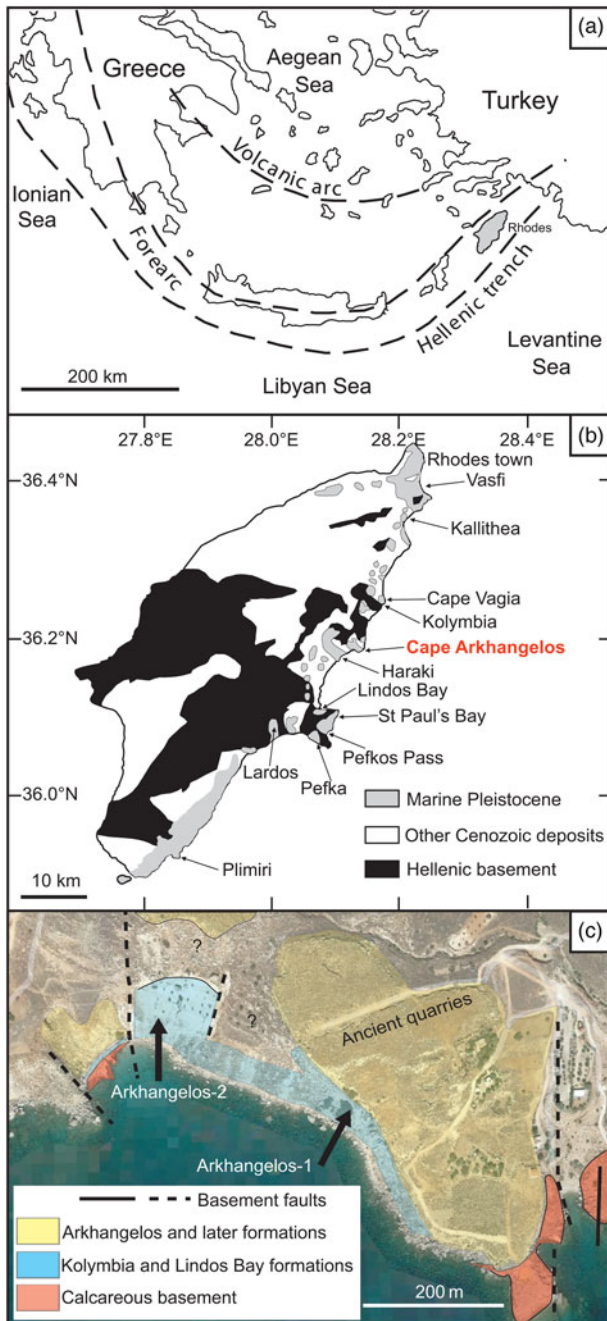
Moissette et al. Fig.1

Figure 1. Simplified maps of the study area. (a) Eastern Mediterranean with simplified tectonic setting (modified from Meulenkamp et al., 1972; Quillévéré et al., 2016). (b) Geology of Rhodes (modified from Mutti et al., 1970; Quillévéré et al., 2016). (c) Schematic geological map of the study area (modified from Google Earth).

In this paper, we study for the first time these atypical deep-sea deposits enriched in transported allochthonous shallow marine components by deciphering their biostratigraphy and by analyzing their paleontological content. We further provide a paleoenvironmental reconstruction that mostly relies on foraminifera and invertebrate faunas (mollusks, bryozoans, and to a lesser degree brachiopods). The emphasis is on deep-water communities since they can be considered as autochthonous, contrary to transported elements (benthic faunas and gravels).

Geological and stratigraphical background

The island of Rhodes, which structurally constitutes the easternmost part of the Aegean sedimentary forearc (Fig. 1A), is made up of nappes that have been accreted as a result of the subduction of Africa beneath Eurasia. Because of the increasing curvature of the forearc along the African/Eurasian plate boundary, the nappes have undergone severe counterclockwise rotations, stretching, faulting, and multiple tilting and vertical motions since the Pliocene (Duermeijer et al., 2000; ten Veen and Kleinspehn, 2002; van Hinsbergen et al., 2007; Cornée et al., 2019). In addition, the concomitant opening of the >4000 m deep Rhodes Basin just east of the island (Woodside et al., 2000; Hall et al., 2009) triggered rapid drowning episodes. Altogether, these tectonics resulted in deposition of Pleistocene marine sediments that have been uplifted and are now patchily exposed inland along the eastern coast of Rhodes (Fig. 1B). There, the Pleistocene marine sediments rest upon a deformed and deeply eroded, mainly calcareous Jurassic to Paleocene basement (Mutti et al., 1970; Meulenkamp et al., 1972; Lekkas et al., 2001). This basement was widely faulted prior to the Pleistocene, generating fault-bounded paleovalleys interpreted as grabens or micro-basins that affected the nature and patchy distribution of the marine Pleistocene deposits (e.g., Hanken et al., 1996; Cornée et al., 2019).

The most severe tectonically driven transgressive–regressive cycle that led to deposition and then uplift of marine sediments now exposed onshore occurred during the Early and Middle Pleistocene. The resulting sedimentary succession of this transgressive–regressive cycle has been qualified as the Rhodes Synthem (Hanken et al., 1996; Titschack et al., 2013; Cornée et al., 2019). Deposition of the Rhodes Synthem (~420 m maximum thickness) started diachronously during the Early Pleistocene (late Gelasian) between ca. 2.0 Ma and ca. 1.9 Ma (Cornée et al., 2006b; Moissette et al., 2016; Quillévéré et al., 2016) with the littoral to lower-offshore transgressive bioclastic clayey limestones of the Kolymbia Formation (Moissette and Spjeldnaes, 1995; Steinthorsdottir et al., 2006). Deposition of the Rhodes Synthem ended during the Middle Pleistocene (Chibanian), ca. 0.46 Ma ago (Cornée et al., 2019), with the regressive red-algal/bryozoan limestones and siliciclastic shallow water deposits of the Cape Arkhangelos Formation, which indicate a major tectonic uplift of Rhodes (van Hinsbergen et al., 2007).

Between the Kolymbia and the Cape Arkhangelos formations, the calcareous to silty hemipelagic blue-gray clays of the Lindos Bay Formation (sometimes associated with deep-sea coral boundstones of the Saint Paul's Bay Formation) constitute the most pronounced tectonic drowning of Rhodes (Hanken et al., 1996; van Hinsbergen et al., 2007). Deposition of the Lindos Bay Formation occurred at upper bathyal depths between ~200 and ~600 m during the Early and Middle Pleistocene with maximum flooding recorded during the Calabrian between ca. 1.9 Ma and ca. 1.0 Ma (Moissette and Spjeldnaes, 1995; Rasmussen and Thomsen, 2005; van Hinsbergen et al., 2007; Quillévéré et al., 2016, 2019; Milker et al., 2017; Agiadi et al., 2018; Cornée et al., 2019). The Lindos Bay Formation clays are predominantly massive and homogenous. However, they often appear bioturbated and sometimes exhibit laminated layers that have been interpreted as shallower extensions of the eastern Mediterranean deep-sea sapropels (Rasmussen and Thomsen, 2005; Quillévéré et al., 2019). Exposures of the Lindos Bay Formation along the eastern coast of Rhodes have been shown to be highly diachronous from section

to section, because of deposition in independent steep and irregular, inherited micro-basins developed at different altitudes (Hanken et al., 1996; Titschack et al., 2013; Quillévéré et al., 2016). Nevertheless, the Lindos Bay Formation has long constituted a key target to resolve the chronostratigraphy of the Lower and Middle Pleistocene of Rhodes. Indeed, the hemipelagic nature of its deposits allowed research on calcareous plankton biostratigraphy, cyclostratigraphy, and magnetostratigraphy of several sections along the eastern coast of the island (Fig. 1B), notably from north to south at Vasfi, Kallithea, Cape Vagia, Kolymbia, Haraki, Lindos Bay, Pefka, Lardos, and Plimiri (Løvlie et al., 1989; Thomsen et al., 2001; Cornée et al., 2006a, b; Titschack et al., 2013; Quillévéré et al., 2016, 2019; Milker et al., 2017, 2019; Eichner et al., 2024; Porz et al., 2024). The chronostratigraphy of these deposits has also benefited from radioisotope dating of (1) a volcaniclastic layer cropping out in its lower part at Kolymbia, Haraki, Pefkos Pass, and Lindos Bay (Cornée et al., 2006b; Quillévéré et al., 2016); and (2) specimens of the deep-water coral *Desmophyllum pertusum* collected in its upper part at Lardos (Titschack et al., 2013; Agiadi et al., 2023).

Material and methods

Sampling and sample processing

During field work in 2019, two sections, termed Arkhangelos-1 (Fig. 2; 36°11'17.31"N, 28°7'28.07"E; 29 m thickness) and Arkhangelos-2 (Fig. 3; 36°11'12.94"N, 28°7'37.15"E; 22 m thickness) were logged and sampled after the outcrop surfaces were refreshed. Thirty-five samples (about 500–1000 g each) were collected, with an average sample spacing of 1.30 m (18 and 17 samples from sections Arkhangelos-1 and Arkhangelos-2, respectively). For micro- and macrofossil analyses, each bulk sample was first oven-dried, then soaked in a dilute solution of 3% hydrogen peroxide (H_2O_2) for about 24 h, and finally washed over a column of sieves (1, 0.5, 0.25, and 0.125 mm). The residues were oven-dried and stored in plastic containers.

Using a stereomicroscope, the gravels and coralline algae were first counted in each residue and their relative abundances were calculated to detect the horizons and samples influenced by the contribution of allochthonous, shallow-water material (Figs. 2 and 3). The micro- (planktonic and benthic foraminifera, bryozoans) and macro- (mollusks, brachiopods) fossils were then observed, identified, counted, and picked. For foraminiferal analyses, a minimum of 300 undamaged or complete specimens of both planktonic and benthic foraminifera from the 125-μm-size fraction were picked per residue (Supplementary Table 1). If a sample contained fewer than 300 undamaged specimens, then all available specimens were counted following the procedure of Schönfeld et al. (2012). For the bryozoans, all specimens available from the residues were picked and identified (Supplementary Table 4). For the mollusks, all complete shells were picked from the >250-μm-size fractions, as well as fragments when they were identifiable to the family, genus, or species levels. Unique fragments were considered (e.g., the apex designated a single specimen for gastropods and scaphopods, and each umbo was assigned to 0.5 specimens for bivalves), following Kowalewski et al. (2002). Some samples did not contain any identifiable material (small-sized fragments).

Qualitative and semi-quantitative analyses of the invertebrate and foraminiferal assemblages were ultimately performed in order to reconstitute the fossil content of these atypical depositional environments, to separate between deep-dwelling and transported taxa, and to obtain a first approximation of the overall conditions that occurred in the water column and the depth of deposition. The qualitative analysis involves identification and description of the species present in a sample, providing insights into diversity and distribution patterns. The faunal analysis adopted a semi-quantitative approach, categorizing occurrences per species as trace, very rare, rare, common, or abundant (Supplementary Tables 2–4), thereby offering a nuanced understanding of species abundance within the assemblages.

The bathymetric zonation used in this study is from van Morkhoven et al. (1986), with the approximate equivalent from Pérès and Picard (1964) for the Mediterranean: inner neritic (= infralittoral; 0–50 m), middle neritic (= upper circalittoral; 50–100 m), outer neritic (= lower circalittoral; 100–200 m), upper slope (= upper bathyal; 200–600 m). Thirty-one deep-water indicators (9 benthic foraminifera, 12 bivalves, 1 scaphopod, and 9 bryozoans) selected from the literature (Fig. 4) among the 336 species identified in this study constitute the basis for the bathymetric subdivisions (Figs. 4 and 5).

Biostratigraphy

Twenty-five unprocessed sediment samples, 12 from Arkhangelos-1 and 13 from Arkhangelos-2, have been investigated for calcareous nannofossil biostratigraphy. Calcareous nannofossils were analyzed in the size fraction 2–30 μm. Smear-slides were studied at 1200× magnification on an Olympus transmitting light microscope, both in crossed-nicols and polarized light. Semi-quantitative analyses of the calcareous nannofossils were achieved by counting 300 specimens per sample in randomly distributed transverses, in order to indicate the abundance patterns and the lowest occurrence (LO), lowest common occurrence (LCO), highest occurrence (HO), and highest common occurrence (HCO) of the stratigraphically significant taxa.

Pleistocene calcareous nannofossil assemblages are dominated by gephyrocapsids and reticulofenestrids. Consequently, due to the taxonomic complexity of the genus *Gephyrocapsa* (Raffi et al., 1993, 2006; Young, 1998), lengths of the coccolith outlines were measured to discriminate between medium (>3.5 to 5.5 μm) and large (>5.5 μm) morphotypes of this genus. The calcareous nannofossil biostratigraphy follows Rio et al. (1990) and Backman et al. (2012), whose zonation schemes have proven applicable for the Pleistocene deposits of the eastern Mediterranean, including the island of Rhodes (Thomsen et al., 2001; Quillévéré et al., 2016). Calibrations of bio-event ages in the eastern Mediterranean are according to Raffi et al. (2006).

Additional biostratigraphic constraints based on planktonic foraminifera rely on a complete inventory of morphospecies and morphotypes in all 35 washed samples in the >125-μm size fraction, following the taxonomic concepts and nomenclature of Kennett and Srinivasan (1983) and Iaccarino et al. (2007). Planktonic foraminiferal bio-event calibrations for the Pleistocene of the Mediterranean Sea come from Lourens et al. (2004), refined by Lirer et al. (2019).

Foraminiferal-based paleodepth estimates

Among the collected samples, only those with no to very rare amounts of gravels (Figs. 2 and 3) were selected for quantitative estimates of the depositional depth since the corresponding levels should contain very few transported (shallow water) benthic
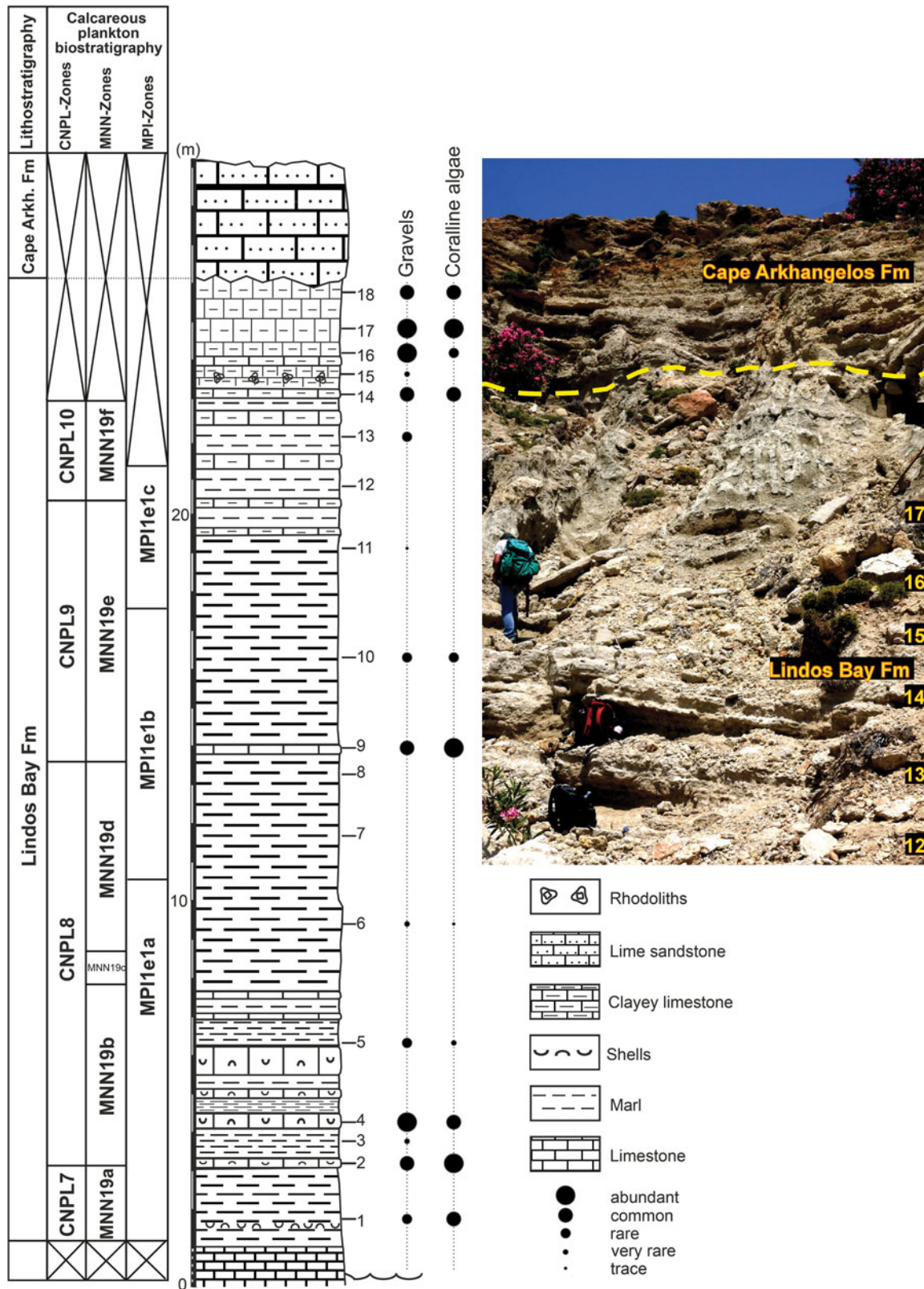
Figure 2. Lithostratigraphy and calcareous plankton (nannofossils and planktonic foraminifera) biostratigraphy of the Cape Arkhangelos-1 section. Tick marks show the locations of collected samples. Points of different sizes indicate the relative abundances of the transported gravels and coralline algae. Calcareous nannoplankton CNPL and MNN zonal schemes by Backman et al. (2012) and Rio et al. (1990), respectively. Planktonic foraminiferal MPle zonal scheme by Lourens et al. (2004).
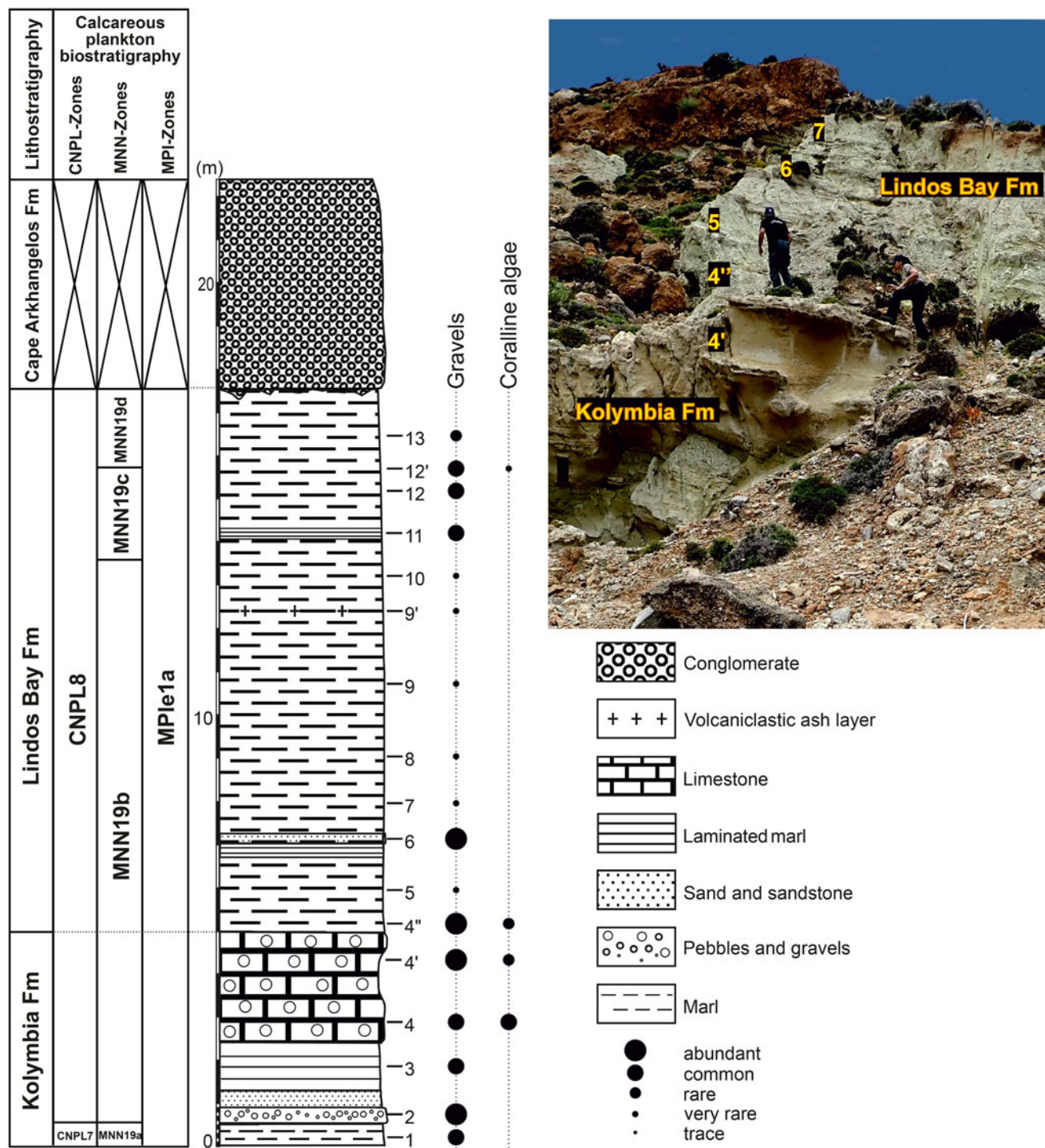
Figure 3. Lithostratigraphy and calcareous plankton (nannofossils and planktonic foraminifera) biostratigraphy of the Cape Arkhangelos-2 section. Tick marks show the locations of collected samples. Points of different sizes indicate the relative abundances of the transported gravels and coralline algae. Calcareous nannoplankton CNPL and MNN zonal schemes by Backman et al. (2012) and Rio et al. (1990), respectively. Planktonic foraminiferal MPle zonal scheme by Lourens et al. (2004).

foraminifera. This fauna was analyzed using representative splits of the >125-µm size fraction. All foraminifera were picked from the split, mounted on faunal slides, and identified. The depositional depth of the sediments of both sections was then assessed by counting the number of planktonic foraminifera (P) relative to the total number of planktonic and benthic foraminifera (P+B), expressed as %P/(P+B) (van der Zwaan et al., 1990). Several

limiting factors play a significant role in controlling benthic and/or planktonic foraminiferal depth habitat, including sensitivity to changes in oxygen levels, food availability (e.g., Jorissen et al., 1995), and preferential dissolution of the planktonic foraminifera (e.g., Berger, 1970; Honjo and Erez, 1978; Thunell and Honjo, 1981; Murray and Alve, 1999; Conan et al., 2002; Zarkogiannis et al., 2022), thus leading to potentially over- or
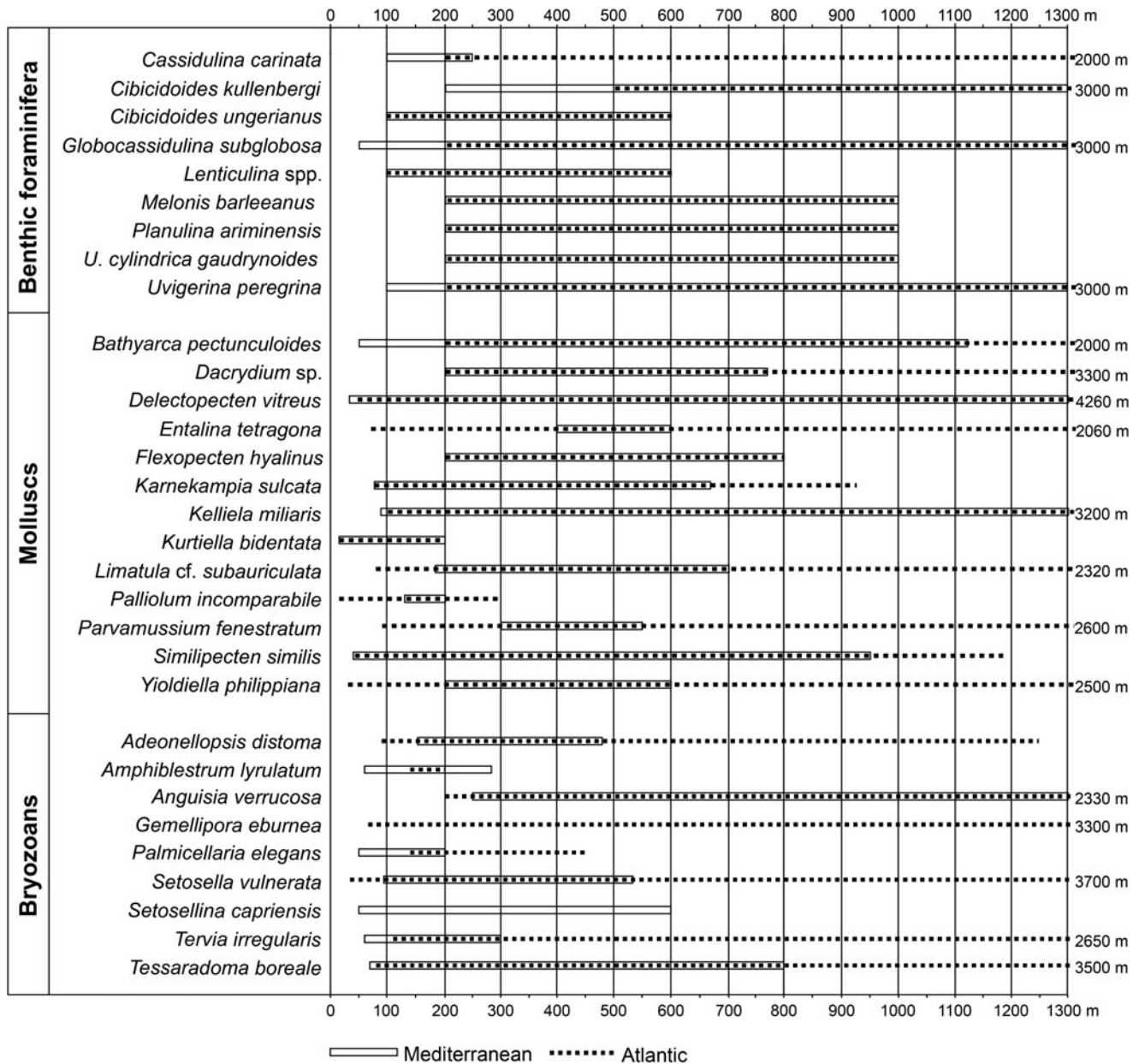
Figure 4. Bathymetric ranges of the deep-water extant species observed in the studied Cape Arkhangelos sections. For benthic foraminifera, bathymetric ranges originate from Parker (1958), Blanc-Vernet (1969), Wright (1978), Parisi (1981), Jorissen (1987), Sprovieri and Hasegawa (1990), Sgarrella and Moncharmont Zei (1993), de Stigter et al. (1998), De Rijk et al. (2000), Seidenkrantz et al. (2000), Kouwenhoven et al. (2003), Drinia et al. (2007), and Milker and Schmiedl (2012). For mollusks, data are from Oliver and Allen (1980), Warén (1989), Oschmann (1991), Peacock (1993), Poppe and Goto (1993), Salas (1996), Salas and Gofas (1997), Koutsoubas et al. (2000), Demir (2003), Petersen (2004), Steiner and Kabat (2004), Dijkstra et al. (2009), Mastrototaro et al. (2010), Studencka et al. (2012), Negri and Corselli (2016), and Krylova et al. (2018). Records for bryozoans include the research of Harmer (1957), Gautier (1962), Prenant and Bobin (1966), Harmelin (1976, 1977), Ryland and Hayward (1977), Hayward and Ryland (1979), Harmelin and d'Hondt (1982), and Rosso (2002).

under-estimated paleodepths. To overcome these limitations, we followed the methodology for collection of specimens originally proposed by van der Zwaan et al. (1990), later modified by van Hinsbergen et al. (2005) and Zachariasse et al. (2021). Van der Zwaan et al. (1990) discarded the benthic genera *Bolivina*, *Bulimina*, *Fursenkoina*, *Globobulimina*, and *Uvigerina* as characteristic of organic-rich and oxygen-deficient environments. Van Hinsbergen et al. (2005) excluded *Uvigerina hispida*, *U. peregrina*, *U. proboscidea*, and *U. semiornata* from the stress markers and used them as depth markers. Moreover, the genera *Cancris*, *Chilostomella*, *Rectuvigerina*, *Stainforthia*, and *Valvulineria* were

added as stress markers. Even though *Hoeglundina elegans* is an epifaunal to shallow-infaunal species, it also was discarded, because water depth is not a factor that affects the occurrence of this species (Pérez-Asensio et al., 2012). The distribution of these species is conceptualized as a function of organic flux and oxygenation, regulating the microhabitats of benthic foraminifera, following the TROX (trophic oxygen) model of Jorissen et al. (1995, 2007). Infaunal species thrive with increased organic flux, especially in oxygen-depleted bottom waters (Jorissen, 1999). Conversely, high percentages of epifaunal species generally indicate well-ventilated, oligotrophic marine conditions.
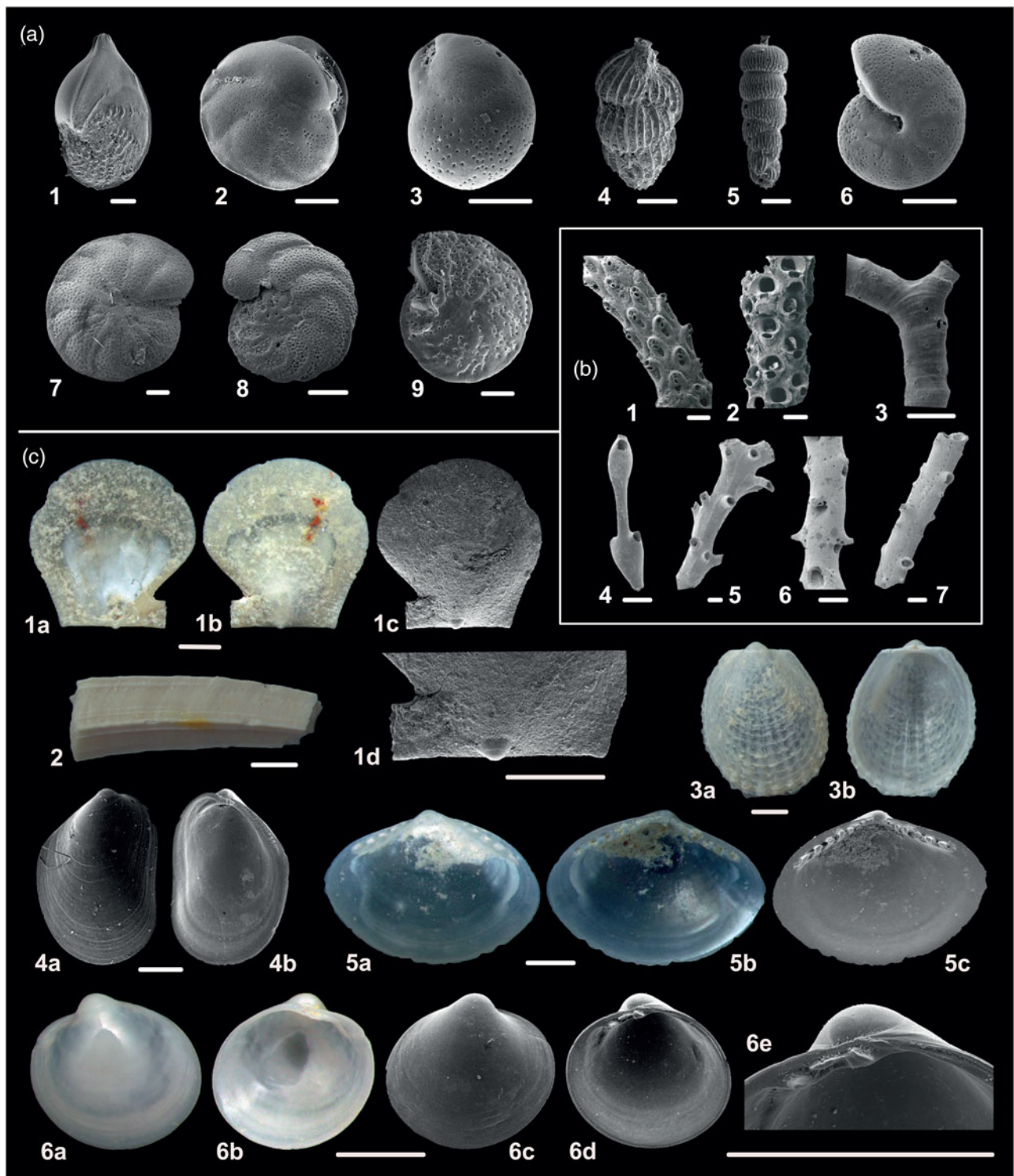
Figure 5. Early Pleistocene deep-water benthic foraminifera, bryozoans, and mollusks collected from the Cape Arkhangelos sections. (a) SEM photomicrographs of benthic foraminifera (scale bars = 100 µm): 1. *Lenticulina* sp., 2. *Cassidulina carinata*, 3. *Globocassidulina subglobosa*, 4. *Uvigerina peregrina*, 5. *Uvigerina cylindrica cylindrica*, 6. *Melonis barleeanus*, 7. *Cibicidoides kullenbergi*, 8. *Planulina ariminensis*, 9. *Cibicidoides ungerianus*. (b) SEM photomicrographs of erect bryozoans (scale bars = 200 µm): 1. *Adeonellopsis distoma*, 2. *Amphiblestrum lyrulatum*, 3. *Anguisia verrucosa*, 4. *Gemellipora eburnea*, 5. *Tervia irregularis*, 6. *Palmicellaria elegans*, 7. *Tessaradoma boreale*. (c) Photographs and SEM photomicrographs of mollusks (scale bars = 500 µm): 1. *Palliolum incomparabile*, 2. *Entalina tetragona*, 3. *Limatula* sp., 4. *Dacrydium* sp., 5. *Yoldiella philippiana*, 6. *Keliella miliaris*.

According to Murray (1991), the inner neritic is characterized by %P/(P+B) values up to 20%, the middle neritic by 20–40%, the outer neritic by 40–70%, and the upper bathyal by more than 70%. The quantitative calculation of foraminiferal data based on %P/(P+B) was checked with qualitative data based on depth-specific benthic marker species, considering their

typical habitats and preferred depths in the Mediterranean region (Fig. 4).

Results

Lithological and faunal characteristics of the sections

In the Cape Arkhangelos area, the Kolymbia Formation rests upon a tectonized basement (Cornée et al., 2019), which consists of folded and metamorphosed limestones of the Aegean nappes. The basement was crosscut by dominantly N–S trending normal faults that created horst and graben structures prior to the Pleistocene. As a consequence, the Kolymbia and Lindos Bay formations exhibit abrupt facies and thickness changes. In the westernmost part of the investigated area (Fig. 1C), these formations display sandy and clayey facies with debris flows that are 4–5 m thick (Cornée al., 2019) and are bounded to the east by a N–S trending fault (Fig. 1C). East of the fault, the formations display marly facies and reach a thickness of about 30 m, indicative of a graben infilling.

The Cape Arkhangelos-1 section (Fig. 2) mostly consists of the clayey and marly deposits of the Lindos Bay Formation. Several limestone (generally clayey) beds occur, notably near the base and at the top where gravels and coralline algae are overall more abundant. Samples 3, 6, 7, 8, 11, 12, and 15 exhibit no to very rare amounts of gravels and/or coralline algae (Fig. 2), and consequently were selected for %P/(P+B) based paleodepth estimates. Bivalve shell accumulations occur in the lowest part of the section and one rhodolith level was found in the upper part. The entire sequence is unconformably overlain by lime sandstones of the Cape Arkhangelos Formation. The benthic foraminifera are represented by about 90 species, which are less abundant and diverse in samples 14, 17, and 18. Forty-two mollusk species have been recognized: 21 bivalves, 20 gastropods (among them 7 holoplanktonic taxa), and 1 scaphopod. The bryozoans are generally abundant and diverse (total: 120 species; average: 25 species/sample), excepted in level 12 where only a few fragments belonging to 2 taxa have been found.

The Cape Arkhangelos-2 section (Fig. 3) first exposes sediments of the Kolymbia Formation: marl (massive or laminated), limestone (with pebbles and gravels), and sandstone beds. The overlying Lindos Bay Formation comprises predominantly massive marly deposits, which are intercalated with a few thin beds of laminated marls and sands. A volcaniclastic ash layer was also observed near the top of the marls of the Lindos Bay Formation. The uppermost conglomerates of the Cape Arkhangelos Formation are separated from the underlying beds by a strong erosional surface. Gravels and/or coralline algae are more abundant in the lower and upper parts of the section. Only samples 5, 7, 8, 9, 9′, and 10 yielded no to very rare amounts of such transported elements (Fig. 3), and consequently were selected for %P/(P+B) based paleodepth estimates. Benthic foraminiferal species diversity is almost like that of the Cape Arkhangelos-1 section, with high numbers of transported components such as *Elphidium* spp. and *Cibicides lobatulus*, accompanied by fewer bathyal elements such as *Cibicidoides* spp., *Planulina ariminensis,* and *Melonis barleeanus* (Fig. 5), together with agglutinated forms. The transport of typical shallow-water foraminifera into deep-sea settings is indicated by the identification of shallow-water foraminiferal species in bathyal sediments and the preservation state of the foraminifera, as well as the examination of sediment grain sizes and assemblage changes. A

mismatch between the grain sizes of bathyal sediments and the typical littoral foraminiferal habitat, along with the sudden appearance of shallow-water species in the bathyal assemblage, may indicate transport. Among the 26 mollusk species found in this section, 18 bivalves have been identified, along with 7 gastropods, and 1 scaphopod. Mostly calcitic shells are preserved in this section and thus pectinid species are predominant, together with a few brachiopods occurring in 5 samples. Bryozoans, totaling 103 species, also were found. Their abundance and average diversity (28 species/sample) are also relatively high, except for samples 5 and 7 (7 and 9 species, respectively).

Apart from the above, various groups of marine organisms are represented in both sections: calcareous algae, sponges (siliceous spicules), solitary corals, tubeworms (ditrupids and serpulids), crustaceans (decapods, ostracods, and barnacles), echinoderms (echinoids mostly, but also ophiuroids and crinoids), and fish (otoliths, teeth, and bone fragments).
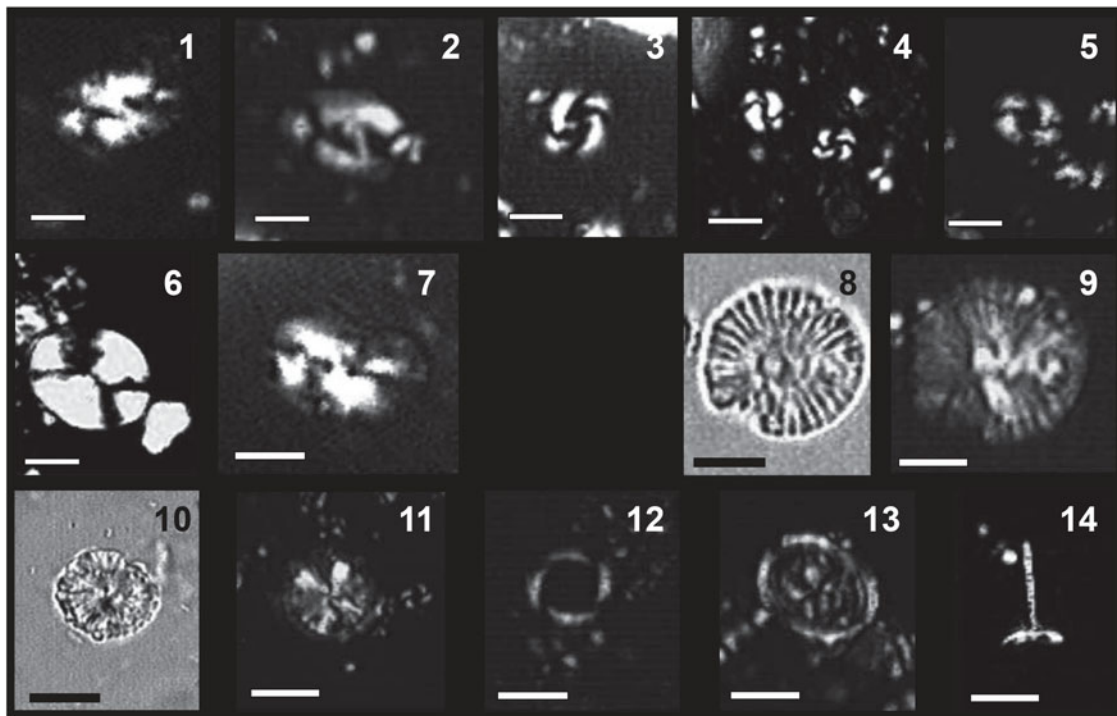
Biostratigraphy

Ten out of the 12 analyzed samples from the Arkhangelos-1 section yielded calcareous nannofossils with preservation ranging from poor to good (samples 14 and 16, collected at the top of the section, were barren). From bottom to top in this section, we identified a biostratigraphic succession encompassing zones and subzones CNPL7–CNPL8 and MNN19a–MNN19f (Fig. 2) based on the LO of medium *Geophyrocapsa* (1.73 Ma), the HO of *Calcidiscus macintyrei* (1.664 Ma), the LO of large *Gephyrocapsa* (1.617 Ma), the HO of *Helicosphaera sellii* (1.256 Ma), the HO of large *Gephyrocapsa* (1.245 Ma), the LCO of *Reticulofenestra asanoi* (1.078 Ma), and the re-entrance datum of medium *Gephyrocapsa* (0.956–0.985 Ma). Additional key information results from the absence of *Discoaster brouweri* (HO at 1.95 Ma) at the base of the section and the continuous common occurrence of *R. asanoi* (HCO at 0.91 Ma) in the uppermost samples that yielded nannofossils.

All samples from the Arkhangelos-2 section yielded calcareous nannofossils with preservation ranging from poor to moderate. From bottom to top in this section, we identified a biostratigraphic succession encompassing zones and subzones CNPL7–CNPL8 and MNN19a–MNN19d (Fig. 3) based on the LO of medium *Gephyrocapsa* (1.73 Ma), the HO of *Calcidiscus macintyrei* (1.664 Ma), and the LO of large *Gephyrocapsa* (1.617 Ma). Additional key information results from the absence of *Discoaster brouweri* (HO at 1.95 Ma) at the base of the section and the continuous occurrence of *Helicosphaera sellii* (HO at 1.256 Ma) at the top. Besides biostratigraphic important taxa (e.g., *Calcidiscus macintyrei*, *Helicosphaera sellii*, *Reticulofenestra asanoi*, along with large and medium-sized *Gephyrocapsa*), some long-ranging nannofossils (e.g., *Calcidiscus leptoporus*, *Helicosphaera carteri*, *Pontosphaera japonica*, *P. multipora*, *Pseudoemiliania lacunosa*, *Rhabdosphaera clavigera*, and *Syracosphaera* spp.) are common throughout the studied successions (Fig. 6).

Planktonic foraminifera are abundant in all analyzed samples and their preservation in the entire Lindos Bay Formation succession of both sections is very good. The base of the Arkhangelos-1 section is characterized by the common occurrence of sinistral *Neogloboquadrina* spp., indicating an age younger than 1.79 Ma (Lourens et al., 2004). This correlates the base of the section with Subzone MPle1a. The absence of sinistral *Neogloboquadrina* spp. in the middle part of the section (samples 7 to 10) correlates

Figure 6. Biostratigraphic important nannoplankton taxa from the studied Arkhangelos sections. (1, 2) *Helicosphaera sellii*. (3) Large *Gephyrocapsa* sp. (4) Medium *Gephyrocapsa* sp. (5) *Reticulofenestra asanoi*. (6) *Pontosphaera japonica*. (7) *Helicosphaera carteri*. (8, 9) *Calcidiscus macintyrei*. (10, 11) *Calcidiscus leptoporus*. (12) *Pseudoemiliania lacunosa*. (13) *Syracosphaera pulchra*. (14) *Rhabdosphaera clavigera*. All microphotographs taken with LM (light microscope) in N+ (crossed-nicols) except (8) and (10) which are in NII (crossed-polarized light); scale bars = 5 μm.

with the paracme interval of these morphotypes, which has been calibrated between 1.37 and 1.21 Ma within the Mediterranean Sea (Subzone MPle1b; Lourens et al., 2004). The FCO of *Globorotalia truncatulinoides excelsa* was also identified in sample 12, indicating an age of 0.934 Ma at the top of Subzone MPle1c (Lourens et al., 2004). In the Arkhangelos-2 section, the common occurrence of sinistral *Neogloboquadrina* spp. is indicative of the interval between the FCO and paracme base (PB) of these morphotypes, corresponding to Subzone MPle1a (part). Other biostratigraphically important taxa found in the Arkanghelos-1 and Arkhangelos-2 sections include *Globoconella inflata* (LO = 2.09 Ma) and *Globorotalia truncatulinoides* (LO = 2.0 Ma).

Overall, the Lindos Bay Formation succession in the study area spans calcareous nannofossil subzones MNN19b–MNN19f (Rio et al., 1990), which correlate with zones CNPL8–CNPL10 (Backman et al., 2012) and planktonic foraminiferal Zone MPle1 (Lourens et al., 2004; Lirer et al., 2019). The Arkhangelos-1 sediments were deposited during the Calabrian, between ca. 1.8 Ma and ca. 0.9 Ma, and those of the Arkhangelos-2 section were deposited during the early Calabrian, probably between ca. 1.8 Ma and ca. 1.6 Ma. The altitude (12.5 m, sample 9′) of the volcaniclastic ash layer found in the Arkhangelos-2 section (Fig. 3) is not in full agreement with the biostratigraphic results. Indeed, a single volcaniclastic ash layer has been found and dated in other Lower Pleistocene sections of the Lindos Bay Formation of Rhodes, namely at Haraki (1.89 ± 0.09 Ma; Cornée et al., 2006b) and at Lindos Bay (1.85 ± 0.08 Ma; Quillévéré et al., 2016). In section Arkanghelos-2, the volcaniclastic ash layer occurs in the 1.73–1.664 Ma interval. Consequently, either its age is slightly younger (at least 70 ka)

than previously suspected, or it correlates with another pyroclastic fallout that occurred later in the Early Pleistocene.

Foraminiferal-based paleodepth estimates

In the 12 selected samples containing no or almost no gravels and coralline algae, all from the marls of the Lindos Bay Formation, % P/(P+B) values range between 16% and 67% in the Arkhangelos-1 section, and between 55% and 75% in the Arkhangelos-2 section (Table 1). Following Murray (1991), the lowermost part of the Arkhangelos-1 section was deposited at upper bathyal depths (around 385 m), then deposition occurred in the outer neritic (between ∼185 m and ∼115 m), and later in the middle neritic (between ∼87 m and ∼65 m) in the uppermost part of the section (Fig. 7). The middle neritic paleodepths may be underestimated in the upper part of the section and deposition may have occurred deeper because of the occurrence of deep-water indicators (for example, the deep-sea mytilid bivalves *Dacrydium* sp. found in sample 11). In the Arkhangelos-2 section, the Lindos Bay Formation sediments were deposited in the upper bathyal zone with a shallowing-upward trend from ∼513 m to ∼254 m (Fig. 8).

Biota

Planktonic foraminifera

Planktonic foraminiferal assemblages consist of a well-diversified fauna containing 14 species and morphotypes: *Globigerinoides ruber, Trilobatus trilobus, Globigerinoides conglobatus, Orbulina universa, Globigerina bulloides, Globorotalia scitula, Globorotalia truncatulinoides, Globoconella inflata, Turborotalita quinqueloba,*

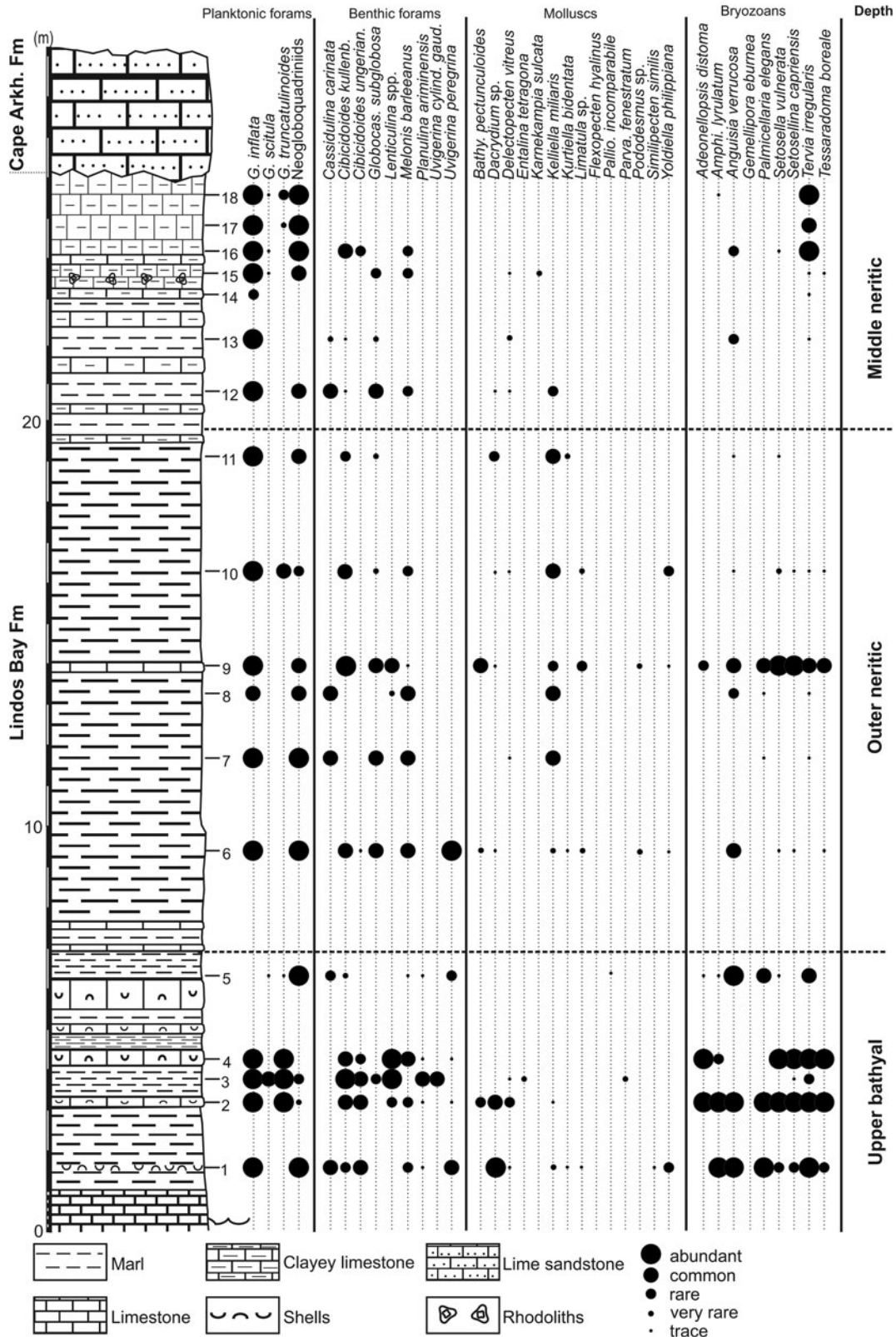| Arkhangelos 1			
Samples	P/(P+B)*100	Depth (m)	Bathymetric zonation
15	25%	87	middle neritic
12	16%	65	middle neritic
11	17%	67	middle neritic
8	33%	115	outer neritic
7	40%	149	outer neritic
6	46%	185	outer neritic
3	67%	385	upper bathyal
Arkhangelos 2			
Samples	P/(P+B)*100	Depth (m)	Bathymetric zonation
10	59%	289	upper bathyal
9	55%	254	upper bathyal
8	73%	487	upper bathyal
7	70%	428	upper bathyal
5	75%	513	upper bathyal

Globoturborotalita apertura, *Globigerinella siphonifera*, *Globigerinita glutinata*, and sinistral and dextral *Neogloboquadrina* spp. Among them, *Globigerinoides ruber*, *Globoconella inflata*, and *Globigerina bulloides* are the most abundant species. Although no significant temporal changes in the planktonic foraminiferal assemblages are observed, *Globoconella inflata*, *Globorotalia scitula*, *Globorotalia truncatulinoides*, and *Neogloboquadrina* spp. highlight distinctive paleoceanographic settings (Figs. 7 and 8). All these deep-dwelling subtropical to subpolar (Hemleben et al., 1989) taxa are usually considered as indicative of relatively cool, mesotrophic water conditions in temperate regions such as the eastern Mediterranean (Rohling et al., 1993; Pujol and Vergnaud-Grazzini, 1995; Rohling et al., 1997; Giamali et al., 2019, 2020, 2021). Their abundance in this setting is mainly controlled by winter convection and vertical mixing (Pujol and Vergnaud-Grazzini, 1995), while, particularly for *Neogloboquadrina* spp., their abundance is mostly associated with the development of the Deep Chlorophyl Maximum (DCM) at the base of the euphotic layer (Rohling and Gieskes, 1989). During early summer, when stratification begins and DCM is absent, they live at the bottom or below the thermocline (Hemleben et al., 1989) and therefore they can be used as indicators of the overall position of the subsurface thermocline (Faul et al., 2000). The co-existence of *Globoconella inflata* and *Globorotalia truncatulinoides* in both sections indicates an isothermal water column throughout the euphotic zone because of the strong seasonal convective mixing (Pujol and Vergnaud-Grazzini, 1995), possibly indicating the presence of intermediate water masses, with the intense action of Levantine Intermediate Waters (LIW) in the south Aegean Sea (Rohling et al., 1997; Kontakiotis, 2016).

Benthic foraminifera

The total benthic foraminiferal data set (Supplementary Table 2) comprises 90 taxonomic units (genera, species, and species groups). The 'Cibicides lobatulus group' (*C. lobatus* and *C. refulgens*) is indicative of inner to middle neritic epifaunal habitats in high-energy settings (Schönfeld, 2002; Louvari et al., 2019). In the two sections, common neritic taxa such as Miliolidae (*Pyrgo depressa*, *Quinqueloculina lamarckiana*, *Quinqueloculina padana*, *Quinqueloculina* spp.), *Reusella spinulosa*, and *Elphidium* spp. (*Elphidium aculeatum*, *Elphidium advenum*, *Elphidium crispum*, *Elphidium macellum*) were most likely transported downslope by turbidity currents (Murray, 2006). Furthermore, sporadic occurrences of taxa with presumed epiphytic growth, such as *Cibicides lobatulus*, asterigerinids, and *Rosalina globularis*, may be attributed to turbidity-current transport or attachment to floating plant material, which then decayed and deposited them (Drinia, 2009). Agglutinated foraminifera, including *Bigenerina nodosaria*, *Textularia agglutinans*, *Textularia conica*, *Textularia gramen*, *Textularia pseudotrochus*, and *Textularia saggitula*, are sporadically present in both sections with no specific environmental preferences identified.

Bathyal taxa such as *Cibicidoides* spp. (including *C. kullenbergi* and *C. ungerianus/pseudoungerianus*), *Planulina ariminensis*, *Melonis barleeanus*, and *Lenticulina* spp. (grouping *L. peregrina* and *L. calcar*) suggest an affinity with finer-grained sediments (e.g., Linke and Lutze, 1993; Pérez-Asensio and Aguirre, 2010). *Cibicidoides* spp. exhibit an upper depth limit within the middle bathyal zone in the Gulf of Mexico (Pflum and Frerichs, 1976). Furthermore, *C. ungerianus* and *C. kullenbergi* are notably abundant deep-water taxa below 100–120 m (Jorissen, 1988; Sgarrella and Moncharmont Zei, 1993). This species group, commonly classified as epifaunal (Jorissen, 1987), shows a preference for well-oxygenated bottoms with high organic carbon fluxes (Woodruff, 1985; Murgese and De Deckker, 2005). *Melonis barleeanus*, which is considered an intermediate-/deep-infaunal species linked to moderately organic-rich sediment (Pflum and Frerichs, 1976; Jorissen, 1987), primarily feeds on degraded organic detritus buried in sediments (Fontanier et al., 2002). The genus *Uvigerina* thrives in low-energy, shallow-infaunal microhabitats rich in organic carbon, often linked to reduced bottom-water oxygen content (Thomas and Gooday, 1996; Fariduddin and Loubere, 1997). *Uvigerina* becomes more abundant with depth, particularly in fine-grained sediments near shelf breaks with local upwelling (Gupta and Srinivasan, 1990; Sen Gupta and Marchain-Castillo, 1993). Among the uvigerinids, *Uvigerina peregrina* is common throughout both sections, with percentages fluctuating between 4% and 30%.

In the lower part of the Arkhangelos-1 section (Fig. 7), the dominance of *Cibicidoides* spp. along with species that typically inhabit deep-water slope settings (e.g., *Planulina ariminensis* and *Siphonina reticulata*), suggests prevailing deep-water conditions (samples 1–4 and 6). This is supported by the common occurrence in sample 3 of *Uvigerina cylindrica gaudrynoides*, a species that inhabits oxygen-deficient and nutrient-rich environments (van der Zwaan, 1982; Drinia et al., 2007). *Uvigerina cylindrica gaudrynoides* typically ranges from the upper to the middle bathyal (200–1000 m), and occasionally occurs as shallow as 150 m and as deep as 1200 m (Haake, 1980; Lutze, 1980; Schiebel, 1992; Schweizer, 2006). In sample 1, the presence of the *Cibicides lobatulus* group and high percentages of Miliolidae and *Elphidium* spp. are attributed to transportation from middle

Figure 7. Cape Arkhangelos-1 section with semi-quantitative abundances of deep-dwelling planktonic foraminifera and deep-water indicators (benthic foraminifera, mollusks, and bryozoans).

to outer neritic settings by turbidity currents, because they co-occur with multiple species of deep-sea invertebrates. Samples 9–10, 13, and 15–18 display high abundances of shallow-water taxa, such as *Asterigerinata mamila, A. planorbis, Neoconorbina terquemi,* and *Rosalina globularis.* These species, commonly found at greater depths in Mediterranean sediments
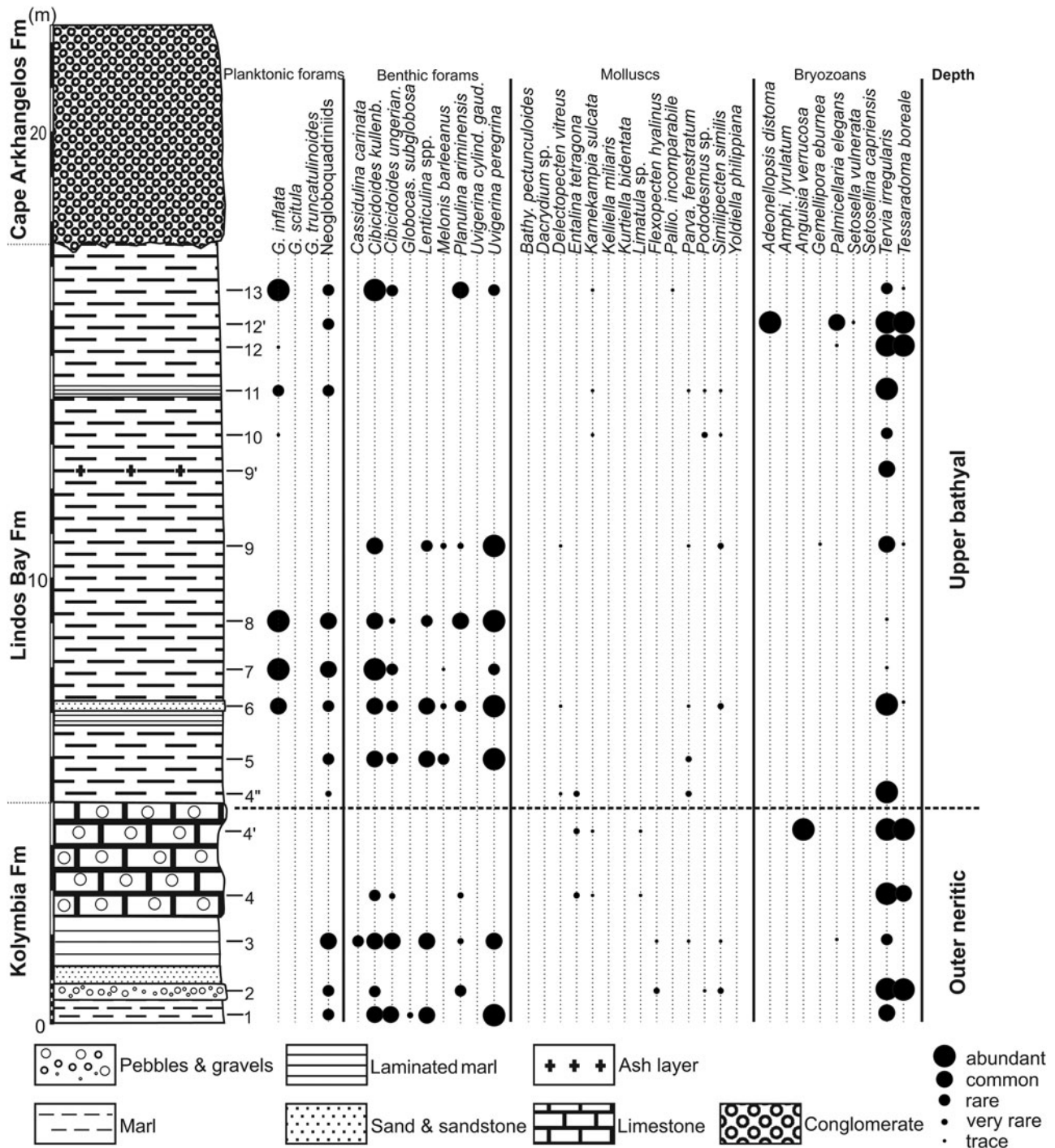
Figure 8. Cape Arkhangelos-2 section with semi-quantitative abundances of deep-dwelling planktonic foraminifera and deep-water indicators (benthic foraminifera, mollusks, and bryozoans).

(e.g., van der Zwaan, 1983; Jorissen, 1987), are considered allochthonous.

In the Arkhangelos-2 section (Fig. 8), *Elphidium* species dominate the benthic foraminiferal assemblages, accompanied by lesser amounts of *Cibicidoides* spp. and *Planulina ariminensis*. The shallow-water preferences of *Elphidium* spp. (Hayward et al., 1997), coupled with the presence of species typical of deep-water habitats, even in small percentages, can be attributed to sediment displacement (e.g., Phleger et al., 1953) or rafting of

plant material, which carried epiphytes into pelagic environments after storms (Sprovieri and Hasegawa, 1990). Common to abundant occurrences of *Uvigerina peregrina*, along with fewer *Cibicidoides* spp. and *Lenticulina* spp. in samples 1, 3, 5–6, and 8–9, support deposition in deep environments (Pflum and Frerichs, 1976; Schnitker, 1979, 1980; Qvale and van Weering, 1985; Gupta and Srinivasan, 1990). The inner to middle neritic epifaunal *Cibicides lobatulus* group is found in samples 3, 5, 6, and 13. High percentages of *Textularia agglutinans* (>40%) and

Elphidiidae (>40%) in samples 2 and 4 suggest either a shallower outer neritic zone or transportation. In sample 10 they indicate transportation. Finally, abundant *Cibicidoides* in samples 7 and 13 indicate an upper bathyal environment.

Mollusks and brachiopods

The total number of mollusk species for the two sections amounts to 83. Bivalves have the highest diversity (38 species; shallow and deep), followed by shallow-water gastropods (35 species), holoplanktonic gastropods (7 species), and deep-water gastropods (2 species). The scaphopods are represented by only 1 (deep-water) species, *Entalina tetragona*. Almost all samples contain fragments of bivalve shells, which are not identifiable at a low taxonomic level; nevertheless, they are mostly fragments of pectinids and anomiids.

The Arkhangelos-1 section (Fig. 7) is characterized by a higher taxonomic diversity than the Arkhangelos-2 section, with a total of 21 species characteristic of deep-water environments: 11 bivalves, 7 holoplanktonic gastropods, 2 bathyal gastropods, and 1 species of scaphopod. Many bivalves (Yoldiidae, Mytilidae, Arcidae or Kelliellidae) are found with preserved aragonitic shells. Minute pectinid bivalves, represented by small fragments and juvenile specimens, are found in most samples. In sample 1, an association of *Dacrydium* sp., *Yoldiella philippiana*, and *Kelliella miliaris* (Fig. 5C) indicates the upper bathyal zone. A second association, recovered in sample 6 and containing *Bathyarca pectunculoides*, *Delectopecten vitreus*, and *Limatula* cf. *L. subauriculata*, is characteristic of outer neritic to upper bathyal depths (180–600 m). In sample 11, the mollusk association is dominated by *Kelliella miliaris*, which co-occurs with *Dacrydium* sp. and *Kurtiella bidentata*, indicating outer neritic depths (up to 200 m). *Yoldiella philippiana* (samples 1, 6, 9, 10) and *Bathyarca pectunculoides* (samples 2, 6, 9) are commonly found at bathyal depths (e.g., Di Geronimo and La Perna, 1997; La Perna, 2003), but in the Atlantic, *Y. philippiana* has been documented from the lower bathyal up to the middle neritic, and in the Mediterranean, *B. pectunculoides* is known from the middle neritic zone and deeper (e.g., Janssen and Krylova, 2014). A varied fauna of holoplanktonic gastropods (Pteropoda and Littorinimorpha) in samples 1–2 and 6–8 includes *Clio pyramidata*, *Creseis* sp., *Thielea* cf. *T. helicoides*, *Atlanta* sp., and *Hyalocyclis* sp. Holoplanktonic gastropods are known from deep environments of 200 m or more (e.g., Berger, 1978; Janssen, 2012; Janssen et al., 2016). Since all the recovered specimens are well preserved, we consider that they have not been transported. The deep-water gastropods *Anatoma crispata* (samples 3, 6, 9, and 10) and *Cornisepta rostrata* (sample 6) further highlight the deep-water depositional settings (Berger, 1978). Sample 3 yielded the scaphopod *Entalina tetragona*, which is known to thrive at depths between 400 and 600 m in the Mediterranean (Fig. 4) (Negri and Corselli, 2016).

In the Arkanghelos-2 section (Fig. 8), eight deep-water mollusk species were found (7 bivalves and 1 scaphopod). The associations of pectinids are characteristic of deep-water environments. Here, six species of deep-water pectinids were recovered, indicating slightly deeper environments than the other taxa, as well as one species of Limiidae (*Limatula* sp.) and the scaphopod *Entalina tetragona*. *Similipecten similis* and *Parvamussium fenestratum* are found together with *Delectopecten vitreus* in upper bathyal environments (sample 6) or with *Flexopecten hyalinus* in outer neritic to upper bathyal

settings (sample 3). The association of *Karnekampia sulcata* and *Limatula* sp. in sample 4 also indicates depths corresponding to the outer neritic or upper bathyal. Sample 4″ recorded a deeper environment (upper bathyal) with the association of *P. fenestratum*, *D. vitreus*, and the scaphopod *Entalina tetragona*. *Karnekampia sulcata* is also found associated with *Palliolum incomparabile* (Fig. 5C) in the uppermost part of the section (sample 13), characterizing an outer neritic to upper bathyal environment.

Numerous samples exhibit transported elements from shallower depths that have been deposited in deeper water. For the Arkhangelos-1 section (samples 6, 9, 10, and 12), holoplanktonic gastropods, such as *Limacina trochiformis* and *Atlanta* sp., are also present. The transported assemblages include the gastropods *Bittium reticulatum*, *Jujubinus* sp., *Alvania* spp., and bivalves of the families Cardiidae (*Papillicardium papillosum*, *Acanthocardia echinata*) and *Timoclea ovata*. The richest assemblage is that of sample 9, followed by sample 6. For sample 12 of the Arkanghelos-2 section, the transported assemblage is dominated by the gastropods *Bittium reticulatum* and *Bittium lacteum*, with other relatively abundant species such as *Clanculus cruciatus*, *Jujubinus* sp., and species of *Alvania*. Shallow-water bivalves include *Arca noae*, *Striarca lactea*, *Hiatella arctica*, *Glycymeris glycymeris*, *Timoclea ovata*, *Ostrea edulis*, and juveniles of the family Veneridae. The deep-water elements of this sample are fragments of characteristic thin-shelled pectinids.

In addition to mollusks, four deep-water brachiopod species are present in the Arkhangelos-2 section, notably in sample 12. These species are *Terebratulina retusa* and *Megerlia truncata*, both living in outer neritic to upper bathyal environments (Logan et al., 2004; Bitner et al., 2013). Other brachiopods (*Macadrevia cranium* and *Platidia anomioides*) also occur in samples 2, 3, 4, 6, and 12. The presence of deep-water brachiopods confirms that the littoral mollusks of sample 12 were transported and deposited into a middle to outer neritic environment.

Bryozoans

About 160 bryozoan species have been identified in the Arkhangelos-1 and Arkhangelos-2 sections. This species richness is far beyond those evinced in other sections of the Lindos Bay Formation, which yielded fewer than 20 species (Moissette and Spjeldnaes, 1995). At Cape Arkhangelos, bryozoans are represented by encrusting (94 species), erect rigid cylindrical (29 species), erect rigid bilaminate (8 species), erect rigid fenestrate (3 species), erect articulated (9 species), nodular (11 species), and free-living discoidal (2 species) morphotypes (Moissette, 2000). The predominance of encrusting forms throughout (with the exception of two species living on small skeletal fragments in deeper, muddy settings) indicates a certain transport from relatively shallow waters (Moissette, 2000), which is confirmed by the occurrence of remains of erect morphotypes often fragmented, some of them also being worn and yellowish.

Apart from numerous eurybathic species, most of the bryozoans are characteristic of shallow to moderate depths (infralittoral to upper circalittoral). Examples of shallow-water inner neritic species are: *Caberea boryi*, *Calpensia nobilis*, *Chaperia annulus*, *Hagiosynodos latus*, *Margaretta cereoides*, and *Savignyella lafontii*. Species living at moderate depths (circalittoral) are more abundant—notably represented by *Cleidochasmidra portisi* (40–130 m), *Hornera frondiculata* (30–130 m), *Microporella verrucosa* (50–120 m), and *Smittina cervicornis* (30–120 m). Only a few

species (7 erect and 2 encrusting) indicate deeper water environments (lower circalittoral to upper bathyal; Figs 7 and 8). They have been chosen as bathymetric indicators (Fig. 4). Scarce accessory taxa (*Adeonellopsis multiporosa*, *Pyripora catenularia*, *Smittoidea marmorea*, and the fossil *Ybselosoecia typica*) also belong to this last group (Moissette and Spjeldnaes, 1995; Moissette et al., 2021).

Extant species constitute the vast majority of the bryozoans found in the Cape Arkhangelos sections. They live in the present-day Mediterranean and eastern Atlantic. Only 12 species are considered as fossil, including *Anoterora persimplex*, *Celleporaria palmata*, *Phoceana pliocenica*, *Smittina canavarii*, *Teuchopora castrocarensis*, and *Ybselosoecia typica*. A few of the shallow-water taxa mostly live in warm-water settings (e.g., *Biflustra savartii*, *Emballotheca*, and *Metrarabdotos*).

Nearly all deeper-water indicators, together with some accessory taxa, occur in abundance at the base of the Arkhangelos-1 section (samples 1–5; Fig. 7), indicating upper bathyal settings (although numerous littoral species/fragments and calcareous algae are also present). The succeeding samples (except sample 9) are much poorer in deeper-water species and contain more abundant shallow-water bryozoans. The upper part of the section is typified by scarce deep-water species, associated with a moderately diverse (except in sample 12 where only 3 species occur) assemblage of shallow-water species. However, the species *Anguisia verrucosa* (Fig. 5), which lives only in the deep sea in both the Mediterranean and the Atlantic (Fig. 4), occurs in multiple samples of the section, up to sample 16. Although the depth of deposition greatly decreased from the base to the top of the section, transportation of shallow-water bryozoans has consequently highly influenced the bryozoan content of the collected samples, with fauna transported from middle-inner neritic depths, even inner neritic near the top of the succession where gravels and coralline algae are fairly abundant. The preservation state of the relatively small number of fragments is generally poor and indicates transportation. Outer neritic to middle neritic environments are therefore inferred for the middle and upper parts of the section.

The Arkhangelos-2 section (Fig. 8) is characterized by the presence of relatively few deep-water indicators found only as relatively rare fragments in a few samples. Even the accessory taxa are represented only by the fossil *Ybselosoecia typica*, which gives barely approximate information on paleobathymetry. Shallow to moderate depths are otherwise indicated by the remaining species and the bryozoans are consequently not especially useful for the detailed study of this section.

Discussion

Essentially deep-water soft bottoms (clayey, more or less silty to sandy) are recorded in the studied material of the Arkhangelos-1 and Arkhangelos-2 sections. The quality of preservation of deep-water skeletal remains is generally high (Fig. 5), whereas allochthonous elements are commonly weathered and fragmented. Following tempests and seismic waves, nearshore sediments received abundant fossils and rock fragments (pebbles, gravels, and sands) from nearby cliffs or rocky bottoms. Most pebbles and gravels are rounded and show borings by clionaid sponges.

Moreover, transported gravels and rare pebbles, together with shells and other skeletal remains such as coralline algae are used as hard substrates (benthic islands) by invertebrates and calcareous algae. Seagrass and seaweeds were probably abundant in

shallow-water environments. This is notably indicated by the occurrence of herbivorous gastropods in a number of beds. This coastal marine vegetation also plays an important role in the transport (horizontal and vertical) of skeletal organisms by floating and rafting.

%P/(P+B) values versus depth taxonomic indicators

Benthic species (i.e., benthic foraminifera) can be used for water depth estimates via transfer functions (e.g., Rossi and Horton, 2009; Milker et al., 2017), although the error is relatively high in deeper waters. In addition, depth reconstructions based on the distribution of benthic organisms can be problematic because many species have a wide bathymetric range over which they can dwell. However, this study aims to overcome these challenges by combining species or groups of species with restricted depth ranges together with ratios between planktonic and benthic foraminifera, %P/(P+B), to estimate water depths. One of the main problems is differentiating between transported (allochthonous) and in-situ (autochthonous) fossil remains. The best criteria are to distinguish pristine from abraded specimens and to assess the ecological requirements of extant species. Eurybathic species predominate throughout both the Arkhangelos-1 and Arkhangelos-2 sections, but are accompanied by stenobathic species, which may have lived either in shallow- or deep-water environments. Moreover, the distinction between true bathyal and circalittoral–bathyal species is often difficult (a number of species having upper depth limits within the neritic zone), and most species show wider and deeper bathymetric ranges in the Atlantic Ocean than in the Mediterranean Sea (Fig. 4).

Consequently, bathymetric variations in the Cape Arkhangelos area appear difficult to estimate precisely because the proportion of transported specimens is notably high throughout most of the deposits and identifying in-situ deep-sea fauna is difficult. In addition, some of the bathymetric indicators lead to contradictory indications. Notably, bryozoan deep-water taxa remain generally uniformly rare, even in levels that are shown to have been deposited in the upper bathyal based on both %P/(P+B) values and benthic foraminiferal and mollusk taxa. The bathymetric variations are also complicated by the fact that while paleodepth estimates based on %P/(P+B) are consistent with the occurrences of deep-water fauna in the lower part of the Arkhangelos-1 section and throughout the Arkhangelos-2 section, the situation appears different in the middle and upper parts of the Arhangelos-1 section. There, paleodepths estimated based on %P/(P+B) values (Table 1) appear likely underestimated, probably because of transportation of shallow-water benthic foraminifera, even in sedimentary levels that were devoid of gravels and coralline algae, and which were therefore the least affected by transportation of allochthonous material.

Consequently, our study confirms that paleodepth estimates based on counts of planktonic foraminifera relative to the total number of foraminifera present issues when applied to deep-sea sediments deposited too close to rugged coastal landforms and indicates that such estimates should be correlated with other bathymetric indicators and parameters. Previous studies (e.g., Schröder-Adams et al., 2008; Hayward et al., 2019) have shown that the inclusion of gravitationally displaced foraminifera in the autochthonous foraminiferal assemblage of deeper parts of the basins alters the paleodepth reconstructions. During dynamic downslope transport, foraminiferal shells can undergo size sorting, abrasion, fragmentation, or dissolution. The distribution of

foraminiferal shells in sediments is influenced by the interplay of factors such as foraminiferal production, sedimentation rate, ocean current transport, destruction (dissolution), and reworking of sediment through downslope transport by earthquakes and re-deposition (Schmuker, 2000). Any index based on foraminiferal material is consequently susceptible to the processes mentioned above. Moreover, previous studies (e.g., Hayward et al., 2019) have already attributed "anomalously" low percentages of planktonic foraminifera to downslope sediment transport. Therefore, the middle and upper parts of the Arkhangelos-1 section, which returned neritic paleodepths based on foraminiferal counts but yielded deep-sea taxonomic indicators, have been influenced by downslope transport resulting in outliers in the %P/(P+B) water-depth relationship.

### Paleoenvironmental conditions in the Arkhangelos area

Upper bathyal paleoenvironmental conditions are first recorded at the base of the Arkhangelos-1 section (samples 1–5; Fig. 7). This is particularly evident in the benthic foraminifera and bryozoan assemblages, represented by relatively abundant deep-water species, and in the occurrence of deep-dwelling species of planktonic foraminifera. The mollusks, apart from *Bathyarca pectunculoides* and *Delectopecten vitreus*, are scarcer. Such an upper bathyal environment is consistent with the ~385 m paleodepth found in sample 3 (Table 1). In the middle part of the section (samples 6–10), deep-water indicators are absent or extremely rare in some levels, especially among the mollusks, but abundance of the bathyal to outer neritic species *Kelliella miliaris* can be common. The species of *Dacrydium* found in this part of the section (Fig. 5) resembles *Dacrydium vitreum* with some differences in the hinge morphology (see Salas and Gofas, 1997, figs. 2–6). In general, the species of *Dacrydium* live at depths below 200 m; only juveniles of *D. hyalinum* have been found at shallower depths on hard-bottom environments (Salas and Gofas, 1997). Benthic foraminifera and bryozoans are better represented, notably by species such as *Cassidulina carinata*, *Melonis barleeanus*, and *Uvigerina peregrina* (benthic foraminifera) or by *Anguisia verrucosa*, *Palmicellaria elegans*, *Setosella vulnerata*, *Setosellina capriensis*, and *Tervia irregularis* (bryozoans). Altogether, these assemblages characterize outer neritic paleoenvironmental conditions. The top of the section (samples 11–18) contains less-diverse and less-abundant deep-water indicators, although some deep-dwelling benthic foraminifera (e.g., *Cibicidoides* spp., *Cassidulina carinata*), bryozoans (*Anguisia verrucosa*), and mollusks (*Dacrydium* sp.) still occur. A middle neritic setting is therefore inferred.

The paleoenvironmental conditions of the Arkhangelos-2 section (Fig. 8) are not easily reconstructed based solely on the taxonomic depth indicators. Compared to Arkhangelos-1 (with approximately the same number of samples), and as previously noted for the bryozoans, fewer species are represented by fewer specimens in fewer samples. Planktonic foraminifera are rare in the lower part of the section (samples 1–4′), but the benthic foraminifera are more diverse and abundant, whereas the mollusks and the bryozoans are represented by relatively few species and specimens. The known depth ranges of the benthic foraminiferal and molluscan depth indicators, together with the lithological features (sandstones and pebble/gravel levels) observed at the base of the section (Figs. 3 and 8) indicate a slightly shallower water depth than above, probably in the outer neritic zone, in agreement with previous studies of the Kolymbia Formation (e.g., Moissette and Spjeldnaes, 1995; Steinthorsdottir et al., 2006). In the middle

and upper parts of the section (samples 4″–13), all samples analyzed for their %P/(P+B) clearly indicate a depth in the upper bathyal zone (Table 1). The mollusks and bryozoans are poorly represented. The benthic foraminifera, which are characterized by fairly abundant specimens belonging to six species indicative of upper bathyal environments (*Cibicidoides kullenbergi*, *C. ungerianus*, *Lenticulina* spp., *Melonis barleeanus*, *Uvigerina peregrina*, *Planulina ariminensis*) in the middle part of the section, even exhibit scanty assemblages in its upper part. Altogether, these features indicate that deposition took place at upper bathyal depth and that it has been less influenced by the transportation of taxa from neritic settings.

Stratigraphic correlations and tectonic implications

Using calcareous nannofossil and planktonic foraminiferal biozones, it is possible to correlate the lower parts of the sections, from Zone CNPL7 to Zone CNPL8 (Fig. 9). Both sections are organized in an overall transgressive–regressive sedimentary cycle above a deformed basement, with the outer neritic deposits of the Kolymbia Formation changing upward into the upper bathyal deposits of the Lindos Bay Formation, and into the middle to inner neritic sediments of the Cape Arkhangelos Formation. A major maximum flooding surface can be recognized in both sections inside Subzone MNN19b (1.73–1.664 Ma) from the deepest faunal content found in both sections (Arkhangelos-1, sample 3; Arkhangelos-2, laminated marls between samples 5 and 6; Table 1). The age of this major maximum flooding event, which is also found elsewhere in Rhodes, was previously estimated to be ca. 1.4 Ma at Pefka (Milker et al., 2019). It is now precisely restricted between 1.73 Ma and 1.664 Ma at Cape Arkhangelos. This result is consistent with the age obtained in the Lefkos Basin at Karpathos Island, 80 km southwest of Rhodes (Moissette et al., 2017) where a major flooding event is also recorded during the 1.730–1.617 Ma interval, with upper bathyal coral buildups resting on a karstified basement. As a consequence, a major Early Pleistocene (early Calabrian) drowning occurred in the eastern Aegean forearc, suggesting a regional event linked to subduction process. In addition, considering a mean age of 1.7 Ma for the maximum flooding zone and the ages of Cornée et al. (2019) for the base of the Kolymbia (2 Ma) and top of the Cape Arkhangelos (0.4 Ma) formations, vertical motions can be roughly estimated to have occurred at Cape Arkhangelos during deposition of the Rhodes Synthem. From 2 Ma to 1.7 Ma, deposits were emplaced at upper bathyal depths of 200–600 m above an emergent basement. During this time interval, deposition was coeval with a minimum rate of drowning of 0.66 mm/yr and a maximum drowning rate of 2 mm/yr, with a mean of ~1.33 mm/yr. This is quite consistent with the rate of 1.7 mm/yr estimated southward at Pefka (Fig. 1) (Cornée et al., 2019; Milker et al., 2019). From 1.7 Ma to ca. 0.4 Ma, facies changed upward from upper bathyal to neritic, and to emergence. A minimum uplift rate of 0.14 mm/yr and a maximum of 0.43 mm/yr, with mean at ~0.28 mm/yr, can be estimated. This rate is much lower than those estimated in other areas of Rhodes (1.3 mm/yr; Cornée et al., 2019). Consequently, the island was probably affected by differential uplift events between 2 Ma and 0.4 Ma, and by repeated, shorter-term, and possibly rapid vertical motions overprinted on the Early Pleistocene regional tectonically forced regressive trend, as already shown along its eastern coast by Milker et al. (2019) and Quillévéré et al. (2019). Noticeably, this average uplift rate is consistent with that
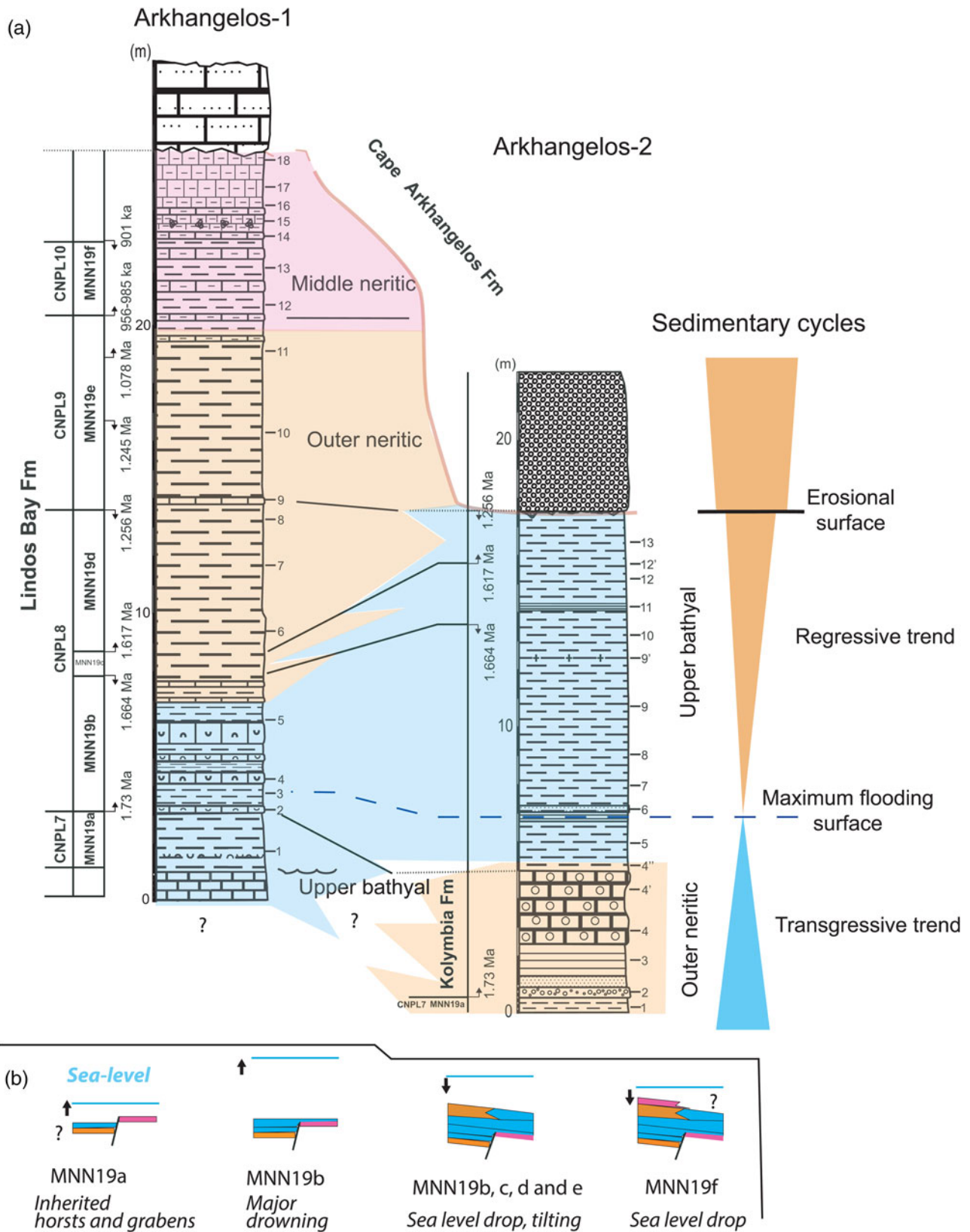
Figure 9. (a) Correlation scheme based on the litho- and biostratigraphy (with calcareous nannofossil bio-event calibrations of Raffi et al., 2006) showing relationships between stratigraphic units of the study area and sedimentary organization. (b) Sedimentary evolution in the study area during the Early Pleistocene (Calabrian) within calcareous nannofossil Subzone intervals. MNN19a: transgression over paleo-relief, with bathyal deposition occurring within former grabens and middle neritic deposition occurring above horsts. Early MNNN19b: major flooding, the entire area was drowned in the upper bathyal zone. MNN19b to MNN19e: tectonically forced regression accompanied by a NW tilting of the area and by deposition of outer neritic deposits above bathyal deposits in the SE. MNN19f: continued regression and middle neritic deposition occurring in the southeastern part of the study area (Arkhangelos-1).

calculated at Karpathos, estimated to be 0.27–0.49 mm/yr (Moissette et al., 2017).

The investigated sections from the Cape Arkhangelos area are only about 300 m from each other but show different facies and thicknesses (Fig. 9). During the time interval corresponding to Zone/Subzone CNPL7/MNN19a, outer neritic sediments of the Kolymbia Formation laterally change to exhibit upper bathyal facies and components at Arkhangelos-1. This indicates that up to the LO of medium *Gephyrocapsa* at 1.73 Ma, the sediments of the Arkhangelos-1 section were deposited in a deep, previously existing paleovalley. Between 1.73 Ma and 1.664 Ma (i.e., during the time interval corresponding to Subzone MNN19b), deposition occurred in the upper bathyal at both locations, indicating a general drowning of the studied area. Finally, between 1.664 Ma and at least 1.256 Ma (i.e., subzones MNN19c and MNN19d), deposition occurred in different settings in the two sections. While deposition changed from upper bathyal to outer neritic at Arkhangelos-1, it remained upper bathyal at Arkhangelos-2. This indicates a northwestward tilting of the micro-basin, in accordance with tilting of the island of Rhodes during the major regression that finally led to the deposition of the Cape Arkhangelos Formation (van Hinsbergen et al., 2007; Cornée et al., 2019).

Consequently, deposition of the Lindos Bay Formation has been controlled partly by tectonic processes: (1) abrupt facies changes resulted from an irregular topography of the calcareous basement during the Early Pleistocene (early Calabrian) transgression, (2) deposits then reached upper bathyal settings during the time interval corresponding to Subzone MNN19b, and (3) northwestward tilting and a regressive trend triggered differential depositional settings during the time interval corresponding to Subzone MMM19d. Later, paleovalleys were infilled by outer to middle neritic sediments, sealing the previous paleorelief irregularities in this part of the basin. Notably, the detrital materials (sands, gravels, pebbles) are consistent with this trend in both studied sections (Figs. 2 and 3) in which they are more abundant in the lower and upper parts of the sections than in their middle part.

Conclusions

During the Early Pleistocene, the paleo-landscape at Cape Arkhangelos comprised a Mesozoic basement of calcareous rocks, which was previously deformed and faulted. The area was divided into blocks responsible for abrupt facies changes during the Early Pleistocene (early Calabrian) transgression. Later, the whole area drowned to bathyal depths with concomitant deposition of hemipelagic sediments of the Rhodes Synthem (marls of the Lindos Bay Formation). These sediments exhibit atypical facies containing both autochthonous (deep-water organisms) and allochthonous (gravels and shallow-water organisms) elements. Finally, an uplift of the investigated area occurred, coeval with differential vertical movements that again triggered abrupt facies changes and then emergence. Our study shows that paleodepth estimates solely based on the number of planktonic foraminifera relative to the total number of foraminifera, %P/(P+B), can be severely biased in such hemipelagic sediments deposited at bathyal depths in the vicinity of coastal areas and steep paleorelief. Consequently, a complete inventory of the foraminifera, bivalve, gastropod, scaphopod, brachiopod, and bryozoan faunas was needed in order to precisely reconstruct the depositional settings. The differentiation between autochthonous and allochthonous fossil components was mostly based on extant species and genera, but also on a few morphological features. Despite a high

abundance of fauna transported from coastal areas, deep-water index benthic taxa were found (as for example *Cibicidoides kullenbergi*, *Melonis barleeanus*, and *Planulina ariminensis* for the foraminifera; *Dacrydium* sp., *Limatula* sp., and *Entalina tetragona* for the mollusks; *Anguisia verrucosa* and *Adeonellopsis distoma* for the bryozoans), and combined with %P/(P+B) values that were estimated only in levels that were devoid of transported gravels and coralline algae. Maximum flooding within the Rhodes Synthem, which is patchily recorded along the eastern coast of Rhodes, is now precisely dated between 1.73 Ma and 1.664 Ma, which is consistent with the age obtained at the island of Karpathos, 80 km southwest of Rhodes.

References

Agiadi, K., Girone, A., Koskeridou, E., Moissette, P., Cornée, J.J., Quillévéré, F., 2018. Pleistocene marine fish invasions and paleoenvironmental reconstructions in the eastern Mediterranean. *Quaternary Science Reviews* 196, 80–99.

Agiadi, K., Quillévéré, F., Nawrot, R., Sommeville, T., Coll, M., Koskeridou, E., Fietzke, J., Zuschin, M., 2023. Palaeontological evidence for community-level decrease in mesopelagic fish size during Pleistocene climate warming in the eastern Mediterranean. *Proceedings of the Royal Society B* 290, 20221994. https://doi.org/10.1098/rspb.2022.1994.

Backman, J., Raffi, I., Rio, D., Fornaciari, E., Pälike, H., 2012. Biozonation and biochronology of Miocene through Pleistocene calcareous nannofossils from low and middle latitudes. *Newsletters on Stratigraphy* 45, 221–244.

Berger, W.H., 1970. Planktonic foraminifera: selective solution and lysocline. *Marine Geology* 8, 111–138.

Berger, W.H., 1978. Deep-sea carbonate: pteropod distribution and the aragonite compensation depth. *Deep Sea Research* 25, 447–452.

Bitner, M.A., Zágoršek, K., Hladilová, T., 2013. Deep-water brachiopod assemblage from the Middle Miocene of Kralice and Oslavou, Moravia, southeastern Czech Republic. *Comptes Rendus Palevol* 12, 81–89.

Blanc-Vernet, L., 1969. Contribution à l'étude des Foraminifères de Méditerranée: relations entre la microfaune et le sédiment; biocoenoses actuelles, thanatocoenoses Pliocènes et Quaternaires. *Recueil des Travaux de la Station Marine d'Endoume* 64, 1–281.

Conan, S.M.H., Ivanova, E.M., Brummer, G.J.A., 2002. Quantifying carbonate dissolution and calibration of foraminiferal dissolution indices in the Somali Basin. *Marine Geology* 182, 325–349.

Cornée, J.J., Moissette, P., Joannin, S., Suc, J.P., Quillévéré, F., Krijgsman, W., Hilgen, F., et al., 2006a. Tectonic and climatic controls on coastal sedimentation: the Late Pliocene–middle Pleistocene of northeastern Rhodes, Greece. *Sedimentary Geology* 187, 159–181.

Cornée, J.J., Münch, P., Quillévéré, F., Moissette, P., Vasiliev, I., Krijgsman, W., Verati, C., Lécuyer, C., 2006b. Timing of Late Pliocene to middle Pleistocene tectonic events in Rhodes (Greece) inferred from magnetobiostratigraphy and ^{40}Ar/^{39}Ar dating of a volcaniclastic layer. *Earth and Planetary Science Letters* 250, 281–291.

Cornée, J.J., Quillévéré, F., Moissette, P., Fietzke, J., López-Otálvaro, G.E., Melinte-Dobrinescu, M.C., Philippon, M., et al., 2019. Tectonic motion in oblique subduction forearcs: insights from the revisited middle and upper Pleistocene deposits of Rhodes, Greece. *Journal of the Geological Society* 176, 78–96.

Demir, M., 2003. Shells of Mollusca collected from the seas of Turkey. *Turkish Journal of Zoology* 27, 101–140.

De Rijk, S., Jorissen, F.J., Rohling, E.J., Troelstra, S.R., 2000. Organic flux control on bathymetric zonation of Mediterranean benthic foraminifera. *Marine Micropaleontology* 40, 151–166.

de Stigter, H.C., Jorissen, F.J., Van der Zwaan, G.J., 1998. Bathymetric distribution and microhabitat partitioning of live (Rose Bengal stained) benthic foraminifera along a shelf to bathyal transect in the southern Adriatic Sea. *Journal of Foraminiferal Research* 28, 40–65.

Dijkstra, H.H., Warén, A., Gudmundsson, G., 2009. Pectinoidea (Mollusca: Bivalvia) from Iceland. *Marine Biology Research* 5, 207–243.

Di Geronimo, I., La Perna, R., 1997. Pleistocene bathyal molluscan assemblages from southern Italy. *Rivista Italiana di Paleontologia e Stratigrafia* 103, 389–426.

Drinia, H., 2009. Palaeoenvironmental reconstruction of the Oligocene Afales Basin, Ithaki Island, western Greece. *Central European Journal of Geosciences* 1, 1–18.

Drinia, H., Antonarakou, A., Tsaparas, N., Dermitzakis, M.D., 2007. Foraminiferal stratigraphy and palaeoecological implications in turbidite-like deposits for the early Tortonian (Late Miocene) of Greece. *Journal of Micropalaeontology* 26, 145–158.

Duermeijer, C.E., Nyst, M., Meijer, P.T., Langereis, C.G., Spakman, W., 2000. Neogene evolution of the Aegean Arc: paleomagnetic and geodetic evidence for a rapid and young rotation phase. *Earth and Planetary Science Letters* 176, 509–525.

Eichner, D., Schmiedl, G., Titschack, J., Triantaphyllou, M., Andersen, N., Forster, N., Milker, Y., 2024. Impact of hydrological changes and vertical motions on Pleistocene marine environments of the eastern coast of the island of Rhodes (Greece). *Palaeogeography, Palaeoclimatology, Palaeoecology* 636, 111980. https://doi.org/10.1016/j.palaeo.2023.111980.

Fariduddin, M., Loubere, P., 1997. The surface ocean productivity response of deeper water benthic foraminifera in the Atlantic Ocean. *Marine Micropaleontology* 32, 289–310.

Faul, K.L., Ravelo, A.C., Delaney, M.L., 2000. Reconstructions of upwelling, productivity, and photic zone depth in the eastern equatorial Pacific Ocean using planktonic foraminiferal stable isotopes and abundances. *Journal of Foraminiferal Research* 30, 110–125.

Fontanier, C., Jorissen, F.J., Licari, L, Alexandre, A., Anschutz, P., Carbonel, P., 2002. Live benthic foraminiferal faunas from the Bay of Biscay: faunal density, composition, and microhabitats. *Deep-Sea Research Part I* 49, 751–785.

Gautier, Y.V., 1962. Recherches écologiques sur les bryozoaires chilostomes en Méditerranée occidentale. *Recueil des Travaux de la Station Marine d'Endoume* 24, 1–434.

Giamali, C., Koskeridou, E., Antonarakou, A., Ioakim, C., Kontakiotis, G., Karageorgis, A.P., Roussakis, G., Karakitsios, V., 2019. Multiproxy ecosystem response of abrupt Holocene climatic changes in the northeastern Mediterranean sedimentary archive and hydrologic regime. *Quaternary Research* 92, 665–685.

Giamali, C., Kontakiotis, G., Koskeridou, E., Ioakim, C., Antonarakou, A., 2020. Key environmental factors controlling planktonic foraminiferal and pteropod community's response to Late Quaternary hydroclimate changes in the South Aegean Sea (Eastern Mediterranean). *Journal of Marine Science and Engineering* 8, 709. https://doi.org/10.3390/jmse8090709.

Giamali, C., Kontakiotis, G., Antonarakou, A., Koskeridou, E., 2021. Ecological constraints of plankton bio-indicators for water column stratification and productivity: a case study of the Holocene North Aegean sedimentary record. *Journal of Marine Science and Engineering* 9, 1249. https://doi.org/10.3390/jmse9111249.

Gupta, A.K., Srinivasan, M.S., 1990. Response of northern Indian Ocean deep-sea benthic foraminifera to global climates during Pliocene–Pleistocene. *Marine Micropaleontology* 16, 77–91.

Haake, F.W., 1980. Benthische Foraminiferen in Oberflächen-Sedimenten und Kernen des Ostatlantiks vor Senegal/Gambia (Westafrika). *Meteor Forschungsergebnisse, Deutsche Forschungsgemeinschaft, Reihe C Geologie und Geophysik, Gebrüder Bornträger, Berlin, Stuttgart* C32, 1–29.

Hall, J., Aksu, A.E., Yaltırak, C., Winsor, J.D., 2009. Structural architecture of the Rhodes Basin: a deep depocentre that evolved since the Pliocene at the junction of Hellenic and Cyprus arcs, eastern Mediterranean. *Marine Geology* 258, 1–23.

Hanken, N.-M., Bromley, R.G., Miller, J., 1996. Plio-Pleistocene sedimentation in coastal grabens, north-east Rhodes, Greece. *Geological Journal* 31, 271–296.

Harmelin, J.G., 1976. Le sous-ordre des Tubuliporina (Bryozoaires Cyclostomes) en Méditerranée. Écologie et systématique. *Mémoires de l'Institut Océanographique* 10, 1–326.

Harmelin, J.G., 1977. Bryozoaires du banc de la Conception (nord des Canaries). Campagne Cineca I du "Jean Charcot". *Bulletin du Muséum National d'Histoire Naturelle, Zoologie* 492, 1057–1076.

Harmelin, J.G., d'Hondt, J.L., 1982. Bryozoaires Cyclostomes bathyaux des campagnes océanographiques de l'"Atlantis II", du "Chain" et du "Knorr" (1967–1972). *Bulletin du Muséum National d'Histoire Naturelle* 4A, 3–23.

Harmer, S.F., 1957. Polyzoa of the Siboga expedition. Part IV. Cheilostomata Ascophora II (Ascophora, except Reteporidae, with addition to part II, Anasca). *Siboga Expedition Reports* 28d, 641–1147.

Hayward, B.W., Sabaa, A.T., Triggs, C.M., 2019. Using foraminiferal test-size distribution and other methods to recognise Quaternary bathyal turbidites and taphonomically-modified faunas. *Marine Micropaleontology* 148, 65–77.

Hayward, B.W., Grenfell, R.H., Pullin, D.A., Reid, C, Hollis, J.C., 1997. Foraminiferal associations in the upper Waitemata Harbour, Auckland, New Zealand. *Journal of the Royal Society of New Zealand* 27, 21–51.

Hayward, P.J., Ryland, J.S., 1979. *British Ascophoran Bryozoans*. Academic Press, London.

Hemleben, C., Spindler, M., Anderson, O.R., 1989. *Modern Planktonic Foraminifera*. Springer-Verlag, New York.

Honjo, S., Erez, J., 1978. Dissolution rates of calcium carbonate in the deep ocean; an in-situ experiment in the North Atlantic Ocean. *Earth and Planetary Science Letters* 40, 287–300.

Iaccarino, S.M., Premoli Silva, I., Biolzi, M., Foresi, L.M., Lirer, F., Turco, E., Petrizzo, M.R., 2007. *Practical Manual of Neogene Planktonic Foraminifera*. Universita di Perugia Press, Perugia, Italy.

Janssen, A.W., 2012. Late Quaternary to Recent holoplanktonic Mollusca (Gastropoda) from bottom samples of the eastern Mediterranean Sea: systematics, morphology. *Bolletino Malacologico* 48, 1–105.

Janssen, R., Krylova, E.M., 2014. Deep-sea fauna of European seas: an annotated species check-list of benthic invertebrates living deeper than 2000 m in the seas bordering Europe. Bivalvia. *Invertebrate Zoology* 11, 43–82.

Janssen, A.W., Sessa, J.A., Thomas, E., 2016. Pteropoda (Mollusca, Gastropoda, Thecosomata) from the Paleocene–Eocene Thermal Maximum (United States Atlantic Coastal Plain). *Palaeontologia Electronica* 19.3.47A. https://doi.org/10.26879/689.

Jorissen, F.J., 1987. The distribution of benthic foraminifera in the Adriatic Sea. *Marine Micropaleontology* 12, 21–48.

Jorissen, F.J., 1988. Benthic foraminifera from the Adriatic Sea; principles of phenotypic variations. *Utrecht Micropaleontological Bulletins* 37, 1–176.

Jorissen, F.J., 1999. Benthic foraminiferal successions across Late Quaternary Mediterranean sapropels. *Marine Geology* 153, 91–101.

Jorissen, F.J., de Stigter, H.C., Widmark, J.G.V., 1995. A conceptual model explaining benthic foraminiferal microhabitats. *Marine Micropaleontology* 26, 3–15.

Jorissen, F.J., Fontanier, C., Thomas, E., 2007. Paleoceanographical proxies based on deep-sea benthic foraminiferal assemblage characteristics. *Developments in Marine Geology* 1, 263–325.

Kennett, J.P., Srinivasan, M.S., 1983. *Neogene Planktonic Foraminifera: A Phylogenetic Atlas*. Hutchinson Ross Publishing Company, Stroudsberg, Pennsylvania.

Kontakiotis, G., 2016. Late Quaternary paleoenvironmental reconstruction and paleoclimatic implications of the Aegean Sea (eastern Mediterranean) based on paleoceanographic indexes and stable isotopes. *Quaternary International* 401, 28–42.

Koutsoubas, D., Tselepidis, A., Eleftheriou, A., 2000. Deep sea molluscan fauna of the Cretan Sea (Eastern Mediterranean): faunal, ecological and zoogeographical remarks. *Senckenbergiana Maritima* 30, 85–98.

Kouwenhoven, T.J., Hilgen, F., van der Zwaan, G.J., 2003. Late Tortonian–early Messinian stepwise disruption of the Mediterranean–Atlantic

connections: constraints from benthic foraminiferal and geochemical data. *Palaeogeography, Palaeoclimatology, Palaeoecology* **198**, 303–319.

Kowalewski, M., Gürs, K., Nebelsick, J.H., Oschmann, W., Piller, W.E., Hoffmeister, A.P., 2002. Multivariate hierarchical analyses of Miocene mollusk assemblages of Europe: paleogeographic, paleoecological, and biostratigraphic implications. *GSA Bulletin* **114**, 239–256.

Krylova, E.M., Sahling, H., Borowski, C., 2018. Resolving the status of the families Vesicomyidae and Kelliellidae (Bivalvia: Venerida), with notes on their ecology. *Journal of Molluscan Studies* **84**, 69–91.

La Perna, R., 2003. The Quaternary deep-sea protobranch fauna from the Mediterranean: composition, depth-related distribution and changes. *Bolletino Malacologico* **39**, 17–34.

Lekkas, E., Danamos, G., Skourtsos, E., Sakellariou, D., 2001. Position of the Middle Triassic Tyros beds in the Gavrovo–Tripolis unit (Rhodes island, Dodecanese, Greece). *Geologica Carpathica* **53**, 37–44.

Linke, P., Lutze, G.F., 1993. Microhabitat preferences of benthic foraminifera – a static concept or a dynamic adaptation to optimize food acquisition? *Marine Micropaleontology* **20**, 215–234.

Lirer, F., Foresi, L.M., Iaccarino, S., Salvatorini, G., Turco, E., Cosentino, C., Sierro, F.J., Caruso, A., 2019. Mediterranean Neogene planktonic foraminifer biozonation and biochronology. *Earth-Science Reviews* **196**, 102869. https://doi.org/10.1016/j.earscirev.2019.05.013.

Logan, A., Bianchi, C.N., Morri, C., Zibrowius, H., 2004. The present-day Mediterranean brachiopod fauna: diversity, life habits, biogeography and paleobiogeography. *Scientia Marina* **68**, 163–170.

Lourens, L.J., Hilgen, F.J., Laskar, J., Shackleton, N.J., Wilson, D.S., 2004. The Neogene Period. In: Gradstein, F.M., Ogg, J.G., Smith, A.G. (Eds.), *A Geologic Time Scale 2004.* Cambridge University Press, pp. 409–440.

Louvari, M.A., Drinia, H., Kontakiotis, G., Di Bella, L., Antonarakou, A., Anastasakis, G., 2019. Impact of latest-glacial to Holocene sea-level oscillations on central Aegean shelf ecosystems: a benthic foraminiferal palaeoenvironmental assessment of South Evoikos Gulf, Greece. *Journal of Marine Systems* **199**, 103181. https://doi.org/10.1016/j.jmarsys.2019.05.007.

Løvlie, R., Støle, G., Spjeldnaes, N., 1989. Magnetic polarity stratigraphy of Pliocene–Pleistocene marine sediments from Rhodos, eastern Mediterranean. *Physics of the Earth and Planetary Interiors* **54**, 340–352.

Lutze, G.F., 1980. Depth distribution of benthic foraminifera on the continental margin off NW Africa. *Meteor Forschungsergebnisse, Deutsche Forschungsgemeinschaft, Reihe C Geologie und Geophysik, Gebrüder Borntraeger, Berlin, Stuttgart* C32, 31–80.

Mastrototaro, F., D'Onghia, G., Corriero G., Matarrese, A., Maiorano, P., Panetta, P., Gherardi, M., *et al.*, 2010. Biodiversity of the white coral bank off Cape Santa Maria di Leuca (Mediterranean Sea): an update. *Deep-Sea Research II* **57**, 412–430.

Meulenkamp, J.E., De Mulder, E.F.J., Van De Weerd, A., 1972. Sedimentary history and paleogeography of the Late Cenozoic of the Island of Rhodos. *Zeitschrift der Deutschen Geologischen Gesellschaft* **123**, 541–553.

Milker, Y., Schmiedl, G., 2012. A taxonomic guide to modern benthic shelf foraminifera of the western Mediterranean Sea. *Palaeontologia Electronica* 15.2.16A. https://doi.org/10.26879/271.

Milker, Y., Weinkauf, M.F.G., Titschack, J., Freiwald, A., Krüger, S., Jorissen, F.J., Schmiedl, G., 2017. Testing the applicability of a benthic foraminiferal-based transfer function for the reconstruction of paleowater depth changes in Rhodes (Greece) during the Early Pleistocene. *PLoS ONE* **12**, e0188447. https://doi.org/10.1371/journal.pone.0188447.

Milker, Y., Jorissen, F., Riller, U., Reicherter, K.R., Titschack, J., Weinkauf, M.F.G., Theodor, M., Schmiedl, G., 2019. Paleo-ecologic and neotectonic evolution of a marine depositional environment in the SE Rhodes (Greece) during the Early Pleistocene. *Quaternary Science Reviews* **213**, 120–132.

Moissette, P., Koskeridou, E., Drinia, H., Cornée, J.J., 2016. Facies associations in warm-temperate siliciclastic deposits: insights from Early Pleistocene eastern Mediterranean (Rhodes, Greece). *Geological Magazine* **153**, 61–83.

Moissette, P., 2000. Changes in bryozoan assemblages and bathymetric variations. Examples from the Messinian of northwest Algeria. *Palaeogeography, Palaeoclimatology, Palaeoecology* **155**, 305–326.

Moissette, P., Spjeldnaes, N., 1995. Plio-Pleistocene deep-water bryozoans from Rhodes, Greece. *Palaeontology* **38**, 771–799.

Moissette, P., Cornée, J.J., Quillévéré, F., Zibrowius, H., Koskeridou, E., López-Otálvaro, G.E., 2017. Pleistocene (Calabrian) deep-water corals and associated biodiversity in the eastern Mediterranean (Karpathos Island, Greece). *Journal of Quaternary Science* **32**, 923–933.

Moissette, P., Antonarakou, A., Kontakiotis, G., Cornée, J.-J., Karakitsios, V., 2021. Bryozoan faunas at the Tortonian–Messinian transition. A palaeoenvironmental case study from Crete Island, eastern Mediterranean. *Geodiversitas* **43**, 1365–1400.

Murgese, D.S., De Deckker, P., 2005. The distribution of deep-sea benthic foraminifera in core tops from the eastern Indian Ocean. *Marine Micropaleontology* **56**, 25–49.

Murray, J.W., 1991. *Ecology and Palaeoecology of Benthic Foraminifera.* Routledge, London.

Murray, J.W., 2006. *Ecology and Applications of Benthic Foraminifera.* Cambridge University Press, New York.

Murray, J.W., Alve, E., 1999. Natural dissolution of modern shallow water benthic foraminifera: taphonomic effects on the palaeoecological record. *Palaeogeography, Palaeoclimatology, Palaeoecology* **146**, 195–209.

Mutti, E., Orombelli, G., Pozzi, R., 1970. Geological studies on the Dodecanese Islands (Aegean Sea). IX. Geological map of the Island of Rhodes (Greece); explanatory notes. *Annales Géologiques des Pays Helléniques* **22**, 79–226.

Negri, M.P., Corselli, C., 2016. Bathyal Mollusca from the cold-water coral biotope of Santa Maria di Leuca (Apulian margin, southern Italy). *Zootaxa* **4186**, 1–97.

Oliver, G., Allen, J.A., 1980. The functional and adaptive morphology of the deep-sea species of the Arcacea (Mollusca: Bivalvia) from the Atlantic. *Philosophical Transactions of the Royal Society of London Series B* **291**, 45–76.

Oschmann, W., 1991. Ecology and bathymetry of the Late Quaternary shelly macrobenthos from bathyal and abyssal areas of the Norwegian Sea. *Senckenbergiana Maritima* **21**, 155–189.

Parisi, E., 1981. Distribuzione dei foraminiferi bentonici nelle zone batiali del Tirreno e del Canale di Sicilia. *Rivista Italiana di Paleontologia e Stratigrafia* **87**, 293–328.

Parker, F.L., 1958. Eastern Mediterranean Foraminifera. *Reports of the Swedish Deep-Sea Expedition* **8**, 217–283.

Peacock, J.D., 1993. Late Quaternary marine Mollusca as palaeoenvironmental proxies: a compilation and assessment of basic numerical data for NE Atlantic species found in shallow water. *Quaternary Science Reviews* **12**, 263–275.

Pérès, J.M., Picard, J., 1964. Nouveau manuel de bionomie benthique de la Mer Méditerranée. *Recueil des Travaux de la Station Marine d'Endoume* **31**, 1–137.

Pérez-Asensio, J.N., Aguirre, J., 2010. Benthic foraminiferal assemblages in temperate coral-bearing deposits from the Late Pliocene. *The Journal of Foraminiferal Research* **40**, 61–78.

Pérez-Asensio, J.N., Aguirre, J., Schmiedl, G., Civis, J., 2012. Messinian palaeoenvironmental evolution in the lower Guadalquivir Basin (SW Spain) based on benthic foraminifera. *Palaeogeography, Palaeoclimatology, Palaeoecology* **326–328**, 135–151.

Petersen, K.S., 2004. The Danish Late Quaternary marine molluscs. *GEUS Bulletin* **3**, 24–97.

Pflum, C.E., Frerichs, W.D., 1976. Gulf of Mexico deep-water foraminifera. *Cushman Foundation for Foraminiferal Research, Special Publication* **14**, 1–125.

Phleger, F.B., Parker, F.L., Peirson, J.F., 1953. North Atlantic foraminifera. In: Pettersson, H. (Ed.), *Reports of the Swedish Deep-Sea Expedition 1947–1948, Sediment Cores from the North Atlantic* **7**, 3–122, Sweden.

Poppe, G.T., Goto, Y., 1993. *European Seashells. Vol. II (Scaphopoda, Bivalvia, Cephalopoda).* Verlag Christa Hemmen, Wiesbaden, Germany, 221 pp.

Porz, A., Zuschin, M., Strotz, L., Koskeridou, E., Simoens, K., Lukic, R., Thivaiou, D., Quillévéré, F., Agiadi, K., 2024. Controls on long-term changes in bathyal bivalve biomass: the Pleistocene glacial–interglacial record in the eastern Mediterranean. *Deep Sea Research Part I: Oceanographic Research Papers* **203**, 104224. https://doi.org/10.1016/j.dsr.2023.104224.

Prenant, M., Bobin, G., 1966. *Bryozoaires. 2. Chilostomes Anasca.* P. Lechevallier, Paris.

Pujol, C., Vergnaud-Grazzini, C., 1995. Distribution patterns of live planktic foraminifers as related to regional hydrology and productive systems of the Mediterranean Sea. *Marine Micropaleontology* **25**, 187–217.

Quillévéré, F., Cornée, J.J., Moissette, P., López-Otálvaro, G.E., van Baak, C., Münch, P., Melinte-Dobrinescu, M.C., Krijgsman, W., 2016. Chronostratigraphy of uplifted Quaternary hemipelagic deposits from the Dodecanese Island of Rhodes (Greece). *Quaternary Research* **86**, 79–94.

Quillévéré, F., Nouailhat, N., Joannin, S., Cornée, J.J., Moissette, P., Lécuyer, C., Fourel, F., Agiadi, K., Koskeridou, E., Escarguel, G., 2019. An onshore bathyal record of tectonics and climate cycles at the onset of the Early–middle Pleistocene transition in the eastern Mediterranean. *Quaternary Science Reviews* **209**, 23–39.

Qvale, G., van Weering, T.C.E., 1985. Relationship of surface sediments and benthic foraminiferal distribution patterns in the Norwegian Channel (northern North Sea). *Marine Micropaleontology* **9**, 469–488.

Raffi, I., Backman, J., Rio, D., Shackleton, N.J., 1993. Plio-Pleistocene nannofossil biostratigraphy and calibration to oxygen isotopes stratigraphies from deep sea drilling project site 607 and ocean drilling program site 677. *Paleoceanography* **3**, 387–408.

Raffi, I., Backman, J., Fornaciari, E., Pälike, H., Rio, D., Lourens, L., Hilgen, F., 2006. A review of calcareous nannofossil astrobiochronology encompassing the past 25 million years. *Quaternary Science Reviews* **25**, 3113–3137.

Rasmussen, T.L., Thomsen, E., 2005. Foraminifera and paleoenvironment of the Plio-Pleistocene Kallithea Bay section, Rhodes, Greece: evidence for cyclic sedimentation and shallow-water sapropels. In: Rasmussen, T.L., Hastrup, A., Thomsen, E. (Eds.), Lagoon to Deep-Water Foraminifera and Ostracods from the Plio-Pleistocene Kallithea Bay Section, Rhodes, Greece. *Cushman Foundation for Foraminiferal Research, Special Publication* **39**, 15–51.

Rio, D., Raffi, I., Villa, G., 1990. Pliocene–Pleistocene calcareous nannofossil distribution patterns in the western Mediterranean. In: Kastens, K.A., Mascle, J., Auroux, C., Bonatti, E., Broglia, C., Channell, J., Curzi, P., Emeis, K.-C., Glaçon, G., *et al.*, *Proceedings of the Ocean Drilling Program, Scientific Results* **107**, 513–533.

Rohling, E.J., Gieskes, W.W.C., 1989. Late Quaternary changes in Mediterranean intermediate water density and formation rate. *Paleoceanography* **4**, 531–545.

Rohling, E.J., Jorissen, F.J., Vergnaud-Grazzini, C., Zachariasse, W.J., 1993. Northern Levantine and Adriatic Quaternary planktic foraminifera; reconstruction of paleoenvironmental gradients. *Marine Micropaleontology* **21**, 191–218.

Rohling, E.J., Jorissen, F.J., Stigter, H.C., 1997. 200 year interruption of Holocene sapropel formation in the Adriatic Sea. *Journal of Micropalaeontology* **16**, 97–108.

Rossi, V., Horton, B.P., 2009. The application of subtidal foraminifera-based transfer function to reconstruct Holocene paleobathymetry of the Po Delta, northern Adriatic Sea. *Journal of Foraminiferal Research* **39**, 180–190.

Rosso, A., 2002. *Amphiblestrum* Gray, 1848 (Bryozoa Cheilostomatida) from the Atlantic–Mediterranean area, with description of a new species. *Journal of Natural History* **36**, 1489–1508.

Ryland, J.S., Hayward, P.J., 1977. *British Anascan Bryozoans*. Academic Press, London.

Salas, C., 1996. Marine bivalves from off the southern Iberian Peninsula collected by the Balgim and Fauna 1 expeditions. *Haliotis* **25**, 33–100.

Salas, C., Gofas, S., 1997. Brooding and non-brooding *Dacrydium* (Bivalvia: Mytilidae): a review of the Atlantic species. *Journal of Molluscan Studies* **63**, 261–283.

Schiebel, R., 1992. Rezente benthische Foraminiferen in Sedimenten des Schelfes und oberen Kontinentalhanges im Golf von Guinea (Westafrika). *Berichte-Reports, Geologisch-Paläontologisches Institut der Universität Kiel* **51**, 126 pp

Schmuker, B., 2000. The influence of shelf vicinity on the distribution of planktic foraminifera south of Puerto Rico. *Marine Geology* **166**, 125–143.

Schnitker, D., 1979. The deep waters of the western North Atlantic during the past 24,000 years, and the re-initiation of the Western Undercurrent. *Marine Micropaleontology* **4**, 265–280.

Schnitker, D., 1980. North Atlantic oceanography as possible cause of Antarctic glaciation and eutrophication. *Nature* **284**, 615–616.

Schönfeld, J., 2002. Recent benthic foraminiferal assemblages in deep high-energy environments from Gulf of Cadiz (Spain). *Marine Micropaleontology* **44**, 141–162.

Schönfeld, J., Alve, E., Geslin, E., Jorissen, F., Korsun, S., Spezzaferri, S., Members of the FOBIMO Group, 2012. The FOBIMO (FOraminiferal BIo-MOnitoring) initiative—towards a standardised protocol for soft-bottom benthic foraminiferal monitoring studies. *Marine Micropaleontology* **94–95**, 1–13.

Schröder-Adams, C.J., Boyd, R., Ruming, K., Sandstrom, M., 2008. Influence of sediment transport dynamics and ocean floor morphology on benthic foraminifera, offshore Fraser Island, Australia. *Marine Geology* **254**, 47–61.

Schweizer, M., 2006. Evolution and molecular phylogeny of *Cibicides* and *Uvigerina* (Rotaliida, Foraminifera). *Geologica Ultraiectina* **261**, 1–167.

Seidenkrantz, M.S., Kouwenhoven, T.J., Jorissen, F.J., Shackleton, N.J., van der Zwaan, G.J., 2000. Benthic foraminifera as indicators of changing Mediterranean–Atlantic water exchange in the Late Miocene. *Marine Geology* **163**, 387–407.

Sen Gupta, B.K., Marchain-Castillo, M.L., 1993. Benthic foraminifera in oxygen-poor habitats. *Marine Micropaleontology* **20**, 183–201.

Sgarrella, F., Moncharmont Zei, M., 1993. Benthic Foraminifera of the Gulf of Naples (Italy): systematics and autoecology. *Bollettino della Società Paleontologica Italiana* **32**, 145–264.

Sprovieri, R., Hasegawa, S., 1990. Plio-Pleistocene benthic foraminifera stratigraphic distribution in the deep-sea record of the Tyrrhenian Sea (ODP Leg 107). In: Kastens, K.A., Mascle, J., Auroux, C., Bonatti, E., Broglia, C., Channell, J., Curzi, P., Emeis, K.-C., Glaçon, G., *et al.*, *Proceedings of the Ocean Drilling Program, Scientific Results* **107**, 429–459.

Steiner, G., Kabat, A.R., 2004. Catalog of species-group names of recent and fossil Scaphopoda (Mollusca). *Zoosystema* **26**, 549–726.

Steinthorsdottir, M., Lidgard, S., Hakansson, E., 2006. Fossils, sediments, tectonics. Reconstructing palaeoenvironments in a Pliocene–Pleistocene Mediterranean microbasin. *Facies* **52**, 361–380.

Studencka, B., Prysyazhnyuk, V.A., Ljul'eva, S.A., 2012. First record of the bivalve species *Parvamussium fenestratum* (Forbes, 1844) from the Middle Miocene of the Paratethys. *Geological Quarterly* **56**, 513–528.

ten Veen, J.H., Kleinspehn, K.L., 2002. Geodynamics along an increasingly curved convergent plate margin: Late Miocene–Pleistocene Rhodes, Greece. *Tectonics* **21**, 1017. https://doi.org/10.1029/2001TC001287.

Thomas, E., Gooday, A.J., 1996. Deep-sea benthic foraminifera: tracers for Cenozoic changes in oceanic productivity? *Geology* **24**, 355–358.

Thomsen, E., Rasmussen, T.L., Hastrup, A., 2001. Calcareous nannofossil, ostracode and foraminifera biostratigraphy of Plio-Pleistocene deposits, Rhodes (Greece), with a correlation to the Vrica section (Italy). *Journal of Micropalaeontology* **20**, 143–154.

Thunell, R.C., Honjo, S., 1981. Calcite dissolution and the modification of planktonic foraminiferal assemblages. *Marine Micropaleontology* **6**, 169–182.

Titschack, J., Joseph, N., Fietzke, J., Freiwald, A., Bromley, R.G., 2013. Record of a tectonically-controlled regression captured by changes in carbonate skeletal associations on a structured island shelf (mid-Pleistocene, Rhodes, Greece). *Sedimentary Geology* **283**, 15–33.

van der Zwaan, G.J., 1982. Paleoecology of Late Miocene Mediterranean foraminifera. *Utrecht Micropaleontological Bulletins* **25**, 1–201.

van der Zwaan, G.J., 1983. Quantitative analyses and the reconstruction of benthic foraminiferal communities. *Utrecht Micropaleontological Bulletins* **30**, 49–69.

van der Zwaan, G.J., Jorissen, F.J., de Stigter, H.C., 1990. The depth dependency of planktonic/benthic foraminiferal ratios: constraints and applications. *Marine Geology* **95**, 1–16.

van Hinsbergen, D.J.J., Kouwenhoven, T.J., van der Zwaan, G.J., 2005. Paleobathymetry in the backstripping procedure: correction for oxygenation effects on depth estimates. *Palaeogeography, Palaeoclimatology, Palaeoecology* **221**, 245–265.

van Hinsbergen, D.J.J., Krijgsman, W., Langereis, C.G., Cornée, J.J., Duermeijer, C.E., van Vugt, N., 2007. Discrete Plio-Pleistocene phases of tilting and counterclockwise rotation in the southeastern Aegean arc

(Rhodos, Greece): Early Pliocene formation of the south Aegean left-lateral strike-slip system. *Journal of the Geological Society, London* **164**, 1133–1144.

van Morkhoven, F.P.C.M., Berggren, W.A., Edwards, A.S., 1986. Cenozoic cosmopolitan deep-water benthic foraminifera. *Bulletin des Centres de Recherches Exploration-Production Elf-Aquitaine* **11**, 1–421.

Warén, A., 1989. Taxonomic comments on some protobranch bivalves from the northeastern Atlantic. *Sarsia* **74**, 223–259.

Woodruff, F., 1985. Changes in Miocene deep-sea benthic foraminiferal distribution in the Pacific Ocean: relationship to paleoceanography. In: Kennett, J.P. (Ed.), The Miocene Ocean: Paleoceanography and Biogeography. *Geological Society of America Memoir* **163**, 131–175.

Woodside, J., Mascle, J., Huguen, C., Volkonskaia, A., 2000. The Rhodes Basin, a post-Miocene tectonic trough. *Marine Geology* **165**, 1–12.

Wright, R., 1978. Neogene paleobathymetry of the Mediterranean based on benthic foraminifers from DSDP Leg 42A. In: Hsu, K.J., Montadert, L., Garrison, R.E., Fabricius, F.H., Mueller, C., Cita, M.B., Bizon, G., *et al.*, *Initial Reports of the Deep Sea Drilling Project* **42**, 837–846.

Young, J.R., 1998. Neogene nannofossils. In: Bown, P.R. (Ed.), *Calcareous Nannofossil Biostratigraphy*. British Micropalaeontology Society Publications Series, Kluwer Academic Publisher, Cambridge, UK, pp. 225–265.

Zachariasse, W.J., Kontakiotis, G., Lourens, L., Antonarakou, A., 2021. The Messinian of Agios Myron (Crete, Greece): a key to better understanding of diatomite formation on Gavdos (south of Crete). *Palaeogeography, Palaeoclimatology, Palaeoecology* **581**, 110633. https://doi.org/10.1016/j.palaeo.2021.110633.

Zarkogiannis, S.D., Iwasaki, S., Rae, J.W.B., Schmidt, M.W., Mortyn, P.G., Kontakiotis, G., Hertzberg, J.E., Rickaby, R.E.M., 2022. Calcification, dissolution and test properties of modern planktonic Foraminifera from the Central Atlantic Ocean. *Frontiers in Marine Sciences* **9**, 864801. https://doi.org/10.3389/fmars.2022.864801.